LMS ADAPTIVE FILTERING APPLIED TO A MICROWAVE ARTERIAL PULSE MONITOR

THESIS

Brian J. Simes
Captain, USAF

AFIT/GE/ENG/88D-45

DEPARTMENT OF THE AIR FORCE
AIR UNIVERSITY
AIR FORCE INSTITUTE OF TECHNOLOGY

Wright-Patterson Air Force Base, Ohio

AFIT/GE/ENG/88D-45

LMS ADAPTIVE FILTERING APPLIED TO A MICROWAVE ARTERIAL PULSE MONITOR

THESIS

Brian J. Simes
Captain, USAF

AFIT/GE/ENG/88D-45

Approved for public release; distribution unlimited

AFIT/GE/ENG/88D-45

LMS ADAPTIVE FILTERING APPLIED TO A MICROWAVE ARTERIAL PULSE MONITOR

THESIS

Presented to the Faculty of the School of Engineering
of the Air Force Institute of Technology
Air University
in Partial Fulfillment of the
Requirements for the Degree of
Master of Science in Electrical Engineering

Brian J. Simes, B.S.
Captain, USAF

December 1988

Preface

I would like to thank the people whose assistance helped make this research possible. First, I would like to thank my thesis advisor, Capt Robert Williams for his many suggestions, helpful advice and support. Maj Glenn E. Prescott for his excellent recommendations on software packages. I would also like to thank Lt Ed Hade of the Acceleration Effects Branch, Armstrong Aerospace Medical Research Laboratory for supplying the microwave transducers. Mr. Bob Durham and Capt Campbell for hardware and software support that made this whole project possible. And finally, I wish to give the greatest thanks and deepest appreciation of all to my wife Barbara, for her kind understanding and support during the many hours of work required for this effort.

Brian J. Simes

Table of Contents

List of Figures

List of Tables

Abstract

A prototype microwave arterial pulse monitor was evaluated and modified. Evaluation test data was collected from the temporal region of human volunteers using the microwave arterial pulse monitor. Three sets of test signals were developed using this test data. These test signals were used to evaluate the feasibility of using a LMS adaptive noise cancellation filter for reduction of noise artifacts observed in the output of the microwave arterial pulse monitor.

A computer program using the LMS algorithm was written and the performance of the LMS filter was evaluated for its effectiveness in removing the unwanted noise. A system model describing the performance characteristics of the test subject-monitor-filter interface is presented.

LMS ADAPTIVE FILTERING APPLIED TO A MICROWAVE ARTERIAL PULSE MONITOR

I. Introduction

Background

Modern high performance aircraft have the capability of causing aircrew loss of consciousness during high +G maneuvers. G-induced loss of consciousness (GLOC) is a serious safety concern and the Air Force is actively conducting research to identify and prevent its occurrence. As part of this effort, the Armstrong Aerospace Medical Research Laboratory (AAMRL) initiated the Biotechnology-Tactical Air Combat (BIOTAC) program in 1983 (13). One of the goals of this program is the development of a GLOC detection system utilizing artificial intelligence technologies and inputs from a variety of aircraft/aircrew sensors.

One of these aircrew sensors is a prototype microwave arterial pulse monitor developed by RCA Sarnoff Laboratories. This device was developed to demonstrate the feasibility of using a microwave transducer for detecting GLOC by indicating the presence/absence of pulses on the temporal artery. Three different prototype versions have been built (5;8;11). All three versions of the sensor

operate in a similar manner, i.e., as an extremely sensitive motion detector. During development, "extremely clear waveforms were obtained at a number of cranial sites... except for [noise] artifacts generated by movement of the subject or external objects relative to the sensor" (5:2). Several techniques have been attempted to reduce the effects of these artifacts including analog filtering and repackaging of the sensor (5:3,18). These techniques have been moderately successful and have reduced the effects of some of the artifacts. Additional work is required to further reduce the effects of these noise artifacts so the sensor can undergo further evaluation as a possible source for reliable GLOC information.

Thesis Problem Statement and Scope

The objective of this thesis is to investigate the feasibility of using a LMS adaptive noise cancellation filter to reduce noise artifacts generated by the AAMRL/RCA microwave arterial pulse monitor. The scope of this research effort consists of three parts, modification of the present monitor's signal conditioning hardware, development of signal/noise test signals for the adaptive filter, and development of a non-real-time LMS adaptive noise cancellation filter to reduce noise artifacts.

Thesis Approach and Assumptions

The approach was to develop an LMS adaptive filter capable of detecting presence/absence of an arterial pulse in the noise environment surrounding the microwave arterial pulse monitor. Experimental data was collected at one G from six subjects using the AAMRL/RCA pulse monitor. Each subject was seated upright in a stationary position and had a resting pulse rate. Data recorded was used to identify monitor modification requirements and to develop the adaptive filter. Filter parameters were selected to account for the wide variety of input signal characteristics observed and were not fine tuned to work only for a specific, narrowly defined or controlled signal set. Because the monitor's output contained no information of "physiological significance... other than the existence of arterial wall movement in response to pulsatile blood flow" (10), work concentrated on detecting this movement and no attempt was made to design the adaptive filter to recover the amplitude or shape information of the pulse monitor's signal output.

The following assumptions were made during this research effort:

1. Data recorded from six subjects at one G with a resting pulse rate provided an adequate test condition for determining the feasibility of using a LMS adaptive filter to reduce noise artifacts.

2. Data collected from the six subjects provided a representative sampling of the types of signals generated by the arterial pulse monitor.

3. Higher pulse rates and G forces will not significantly alter the performance of the adaptive filter.

4. Sensor noise generated by background movement can be significantly reduced by a separate effort aimed at sensor redesign or improved shielding/mounting techniques.

The above assumptions were kept to a minimum and were selected to provide a realistic environment to assess the adaptive filter, its actual performance and feasibility of its use for noise cancellation.

Thesis Organization

This chapter has provided a brief background on the AAMRL/RCA microwave arterial pulse monitor, a statement of the objective of this thesis, an outline of the tasks performed and a list of assumptions used in the performance of this research effort. The following chapters in this thesis will address the experimental setup and procedures used for the collection of data, a description and evaluation of the arterial pulse monitor, test signal development, the LMS adaptive filter and its performance, the subject-monitor-filter model and finally the conclusions and recommendations.

II. Experimental Setup and Procedure

Introduction

In the previous chapter, a brief background of the AAMRL/RCA microwave arterial pulse monitor was discussed along with the thesis objective and scope. This chapter will continue with the experimental setup and procedures used to record evaluation data for the pulse monitor and test data for the adaptive filter.

Experimental Setup

The equipment used in the experimental setup was selected to provide for a flexible data acquisition and processing system capable of meeting the following requirements:

1. Accept input data with a wide range of amplitudes and frequencies from multiple sources.
2. Provide simultaneous multi-channel analog/digital conversion of input data at variable sample rates.
3. Provide real-time acquisition and display of the multi-channel data.
4. Provide a post acquisition data processing capability to selectively edit and store the data for subsequent analysis or filter test use.

Equipment. The equipment used included the following:

1. A Wavetek model 852 dual 8-pole low pass filter.
2. A Zenith Z-248 personal computer with peripheral units including:
    a. A Metra-Byte Dash-16F 12 bit analog/digital converter I/O expansion board configured for +/-5v bipolar operation.

b. A DATAQ WFS-200PC waveform scroller board.

c. An INTEL 80287 math coprocessor chip.

3. An electrocardiogram (ECG).

4. Two AAMRL/RCA microwave arterial pulse monitors.

Software. The software used included the following:

1. DATAQ Instruments' CODAS data acquisition/playback program for use with the DATAQ WFS-200PC waveform scroller board and the Metra-Byte Dash-16F A/D converter board.

2. DSP Development Corporation's DADisP signal analysis software for use in processing and analyzing recorded data, and generating test signals for the adaptive filter.

3. Borland International's Turbo Pascal 4.0 for use in writing the adaptive filter program.

Setup Configuration. Three different experimental setup configurations were used to record data for use in the thesis. A composite diagram of the three setups is shown in Figure 1. All configurations shared in common the elements of the Z-248 computer and the low pass filter. Differences between each setup included the type, quantity and mounting location of the input sensors; amplification levels, filter cut-off frequencies and sampling rates. The three configurations were used to record data for different purposes. The first configuration was used to gather data for modification and evaluation of the arterial pulse monitor, the second for recording data for development and test of the adaptive filter, and the third for recording ECG/pulse monitor correlation data.

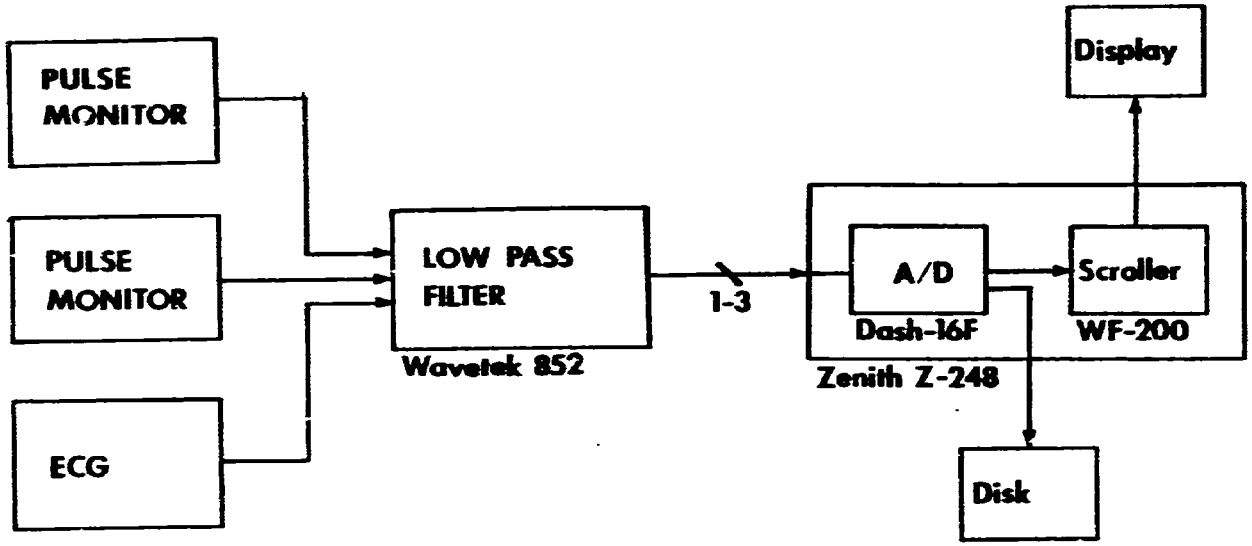

Figure 1. Experimental Setup

Pulse Monitor Evaluation Setup. The pulse monitor evaluation setup was used to identify and evaluate the characteristics of the pulse monitor for use in determining the monitor's modification requirements and later use in the development of experimental procedures. The pulse monitor evaluation setup was not a fixed design and was modified iteratively as the evaluation progressed. The configuration initially contained a single arterial pulse monitor, a low pass (anti-aliasing) filter and the Z-248 system configuration as shown in Figure 1. The arterial pulse monitor(s) used for this setup (and thesis) were removed from the flight helmet obtained from the Multiple Sensor Arterial Pulse Monitor Program (5). The monitor evaluated was initially unmodified with the exception of mounting the monitor's microwave sensor inside the earpiece on a pair of headphones. The headphones were used to facilitate placement of the sensor at multiple locations in the temporal region of each test subject and to simulate a conformally fitted flight helmet recommended for sensor evaluation by Mawhinney (5:6). As evaluation progressed, the sensor was modified by attaching a layer of ECCOSORB AN-P microwave absorbing foam to the side and back of the sensor to reduce the effects of noise artifacts generated by background movement near the test subjects. Additional modifications for the pulse monitor evaluation setup occurred iteratively and included the addition of a second

arterial pulse monitor (with foam shielded sensor), optimization of the pulse monitor/low pass filter amplifier gain levels, filter cut-off frequencies and sampling rates. The optimum amplifier gain level was determined based on minimizing occurrence of amplifier saturation and obtaining the largest pulse monitor's pulse signal output levels possible. Amplifier gain levels evaluated varied from a high of 8635 to a low of 451 with the gain level of 1845 selected as optimum. The optimum low pass filter cut-off frequency was determined based on maximizing the monitor's signal-to-noise ratio while preserving the pulse signal peaks of the monitor's output. The low pass filter cut-off frequencies varied between 500 and 1.0 Hz with the value of 9.0 Hz selected as optimum. Sampling rates were chosen to comply with the Nyquist sampling criterion where the sampling rate is chosen to be at least twice the filter cut-off frequency. A summary of the pulse monitor evaluation experimental setup is listed in Table 1. The final (optimum) configuration used in the pulse monitor evaluation setup was the same configuration used for the pulse monitor data recording setup.

Pulse Monitor Data Recording Setup. The pulse monitor data recording setup was used to determine the optimum position for recording pulse monitor sensor data for latter use in developing test signals for evaluation of the adaptive filter. The configuration setup was a fixed design

Table 1. Pulse Monitor Evaluation Experimental Setup

	Value Range	Optimum
# of Sensors	1 - 2	N/A
Gain	451 - 8635	1845
Filter Cut-off Frequency	1.0 - 500 Hz	9.0 Hz
Sample Rate	10 - 1000 Hz	20 Hz

and did not change during the data recording process. The pulse monitor data recording configuration setup consisted of two modified arterial pulse monitors, a pair of low pass (anti-aliasing) filters and the Z-248 system configuration shown in Figure 1. The pulse monitor/low pass filter amplifier gain levels, filter cut-off frequencies and sampling rates are listed in Table 2. These values were the same used for the optimum pulse monitor evaluation setup.

Table 2. Pulse Monitor Data Recording Setup

	Value
# of Sensors	2
Gain	1845
Filter Cut-off Frequency	9.0 Hz
Sample Rate	20 Hz

ECG/Pulse Monitor Setup. The ECG/pulse monitor setup was used to obtain information on the correlation between the occurrence of the ECG's E-wave and the pulse monitor's peak pulse wave. The ECG/pulse monitor setup contained a single modified arterial pulse monitor, an ECG, two low pass (anti-aliasing) filters and the Z-248 system shown in Figure 1. The configuration setup was a fixed design and was not changed during the data collection process. Amplifier gain level for the pulse monitor was set at 184.5 and the gain level for the low pass filters were set at 10.0 (same as the previous two setups). The low pass filter cut-off frequencies were adjusted to 18 Hz to accommodate the wider frequency spectrum of the ECG and the sampling rate was likewise changed to satisfy Nyquist sampling criterion. A summary of the ECG/pulse monitor experimental setup is listed in Table 3.

Table 3. ECG/Pulse Monitor Experimental Setup

	Value
# of Sensors	1
# of ECGs	1
Sensor Gain	184.5
Filter Gain	10
Filter Cut-off Frequency	18 Hz
Sample Rate	40 Hz

Experimental Procedure

The experimental procedure consisted of seating a volunteer subject in an upright position in a chair, attaching one or two pulse monitor sensors to the subject's temporal region and recording output data from the monitor. For the ECG/pulse monitor data setup, an ECG was used as a data source and was substituted for one of the pulse monitors. Data was collected at one G from six subjects at their resting pulse rates. Each subject was instructed to minimize head movements during the recording of data to reduce noise artifacts caused by motion of the sensor relative to nearby objects. During the experiment, each subject was instructed to perform a series of facial muscular movements designed to generate pulse monitor noise artifacts. The types of facial muscular movements evaluated included speaking, face flexing and various types of jaw/eye movement. These types of movements were used because they were found during initial analysis to be representative of the variety of noise artifacts generated by the pulse monitor. Muscular movement caused by speaking was standardized by having each subject recite the same phrases. The results of each experiment was recorded on floppy disks and logged in on data collection sheets. Recorded data was tagged with event markers to ease identification during subsequent analysis. Copies of the data collection sheets used for the experiment are contained in Appendix A.

III. AAMRL/RCA Arterial Pulse Monitor

Introduction

Previous chapters have provided background information and discussed the experimental setups and procedures used to evaluate the arterial pulse monitor. This chapter will continue with a detailed description of the arterial pulse monitor, its prototype configuration, operation, modification and evaluation.

Arterial Pulse Monitor Prototype (5;6;10)

The AAMRL/RCA microwave arterial pulse monitor is a miniaturized microwave motion sensor designed to detect the pulsatile movement of arteries located close to the surface of the skin. The arterial pulse monitor consists of a motion detection sensor and a remotely located amplifier/processor module.

Motion Detection Sensor. The motion detection sensor is a low power microwave oscillator designed to operate at 2.45 GHz. It is constructed from a N-P-N bipolar oscillator transistor (Hewlet Packard HXTR-4101) mounted inside a circular stamped brass housing 27-mm in diameter and 8-mm thick. A strip antenna is attached to the transistor and enclosed in the oscillator housing by a brass cover containing a machined slot for the antenna. A circular washer of R-F absorptive material is attached to the antenna side of the brass cover to reduce microwave leakage.

Interface to the amplifier/processor module is accomplished via a small diameter two wire shielded cable. The schematic diagram of the motion detection sensor is shown in Figure 2.

Motion Detector Sensor Operation. The motion detector sensor operates by detecting minute changes in the impedance of its antenna caused by changes in the positions of objects relative to the sensor (8:7-8). As the sensor's antenna changes impedance, the loading of the microwave oscillator is altered and a change in its operating current occurs. This change in operating current can be detected by the arterial pulse monitor's amplifier/processor module and amplified to produce a voltage output indicative of movement. The motion detector sensor is extremely sensitive to motion and can detect the pulsatile wall movement of superficially located arteries such as the temporal, occipital, brachial, radial, or femoral (10;11:6).

Amplifier/Processor Module. The amplifier/processor module is a two stage amplifier containing a low pass filter, a full wave rectifier and a dual peak-detector comparator. A block diagram of the amplifier/processor module is shown in Figure 3.

Amplifier/Filter Operation. The amplifier/filter section of the module is constructed from a single instrumentation amplifier (Burr-Brown INA104). This instrumentation amplifier provides the capability of amplifying weak signals at high input impedance levels while

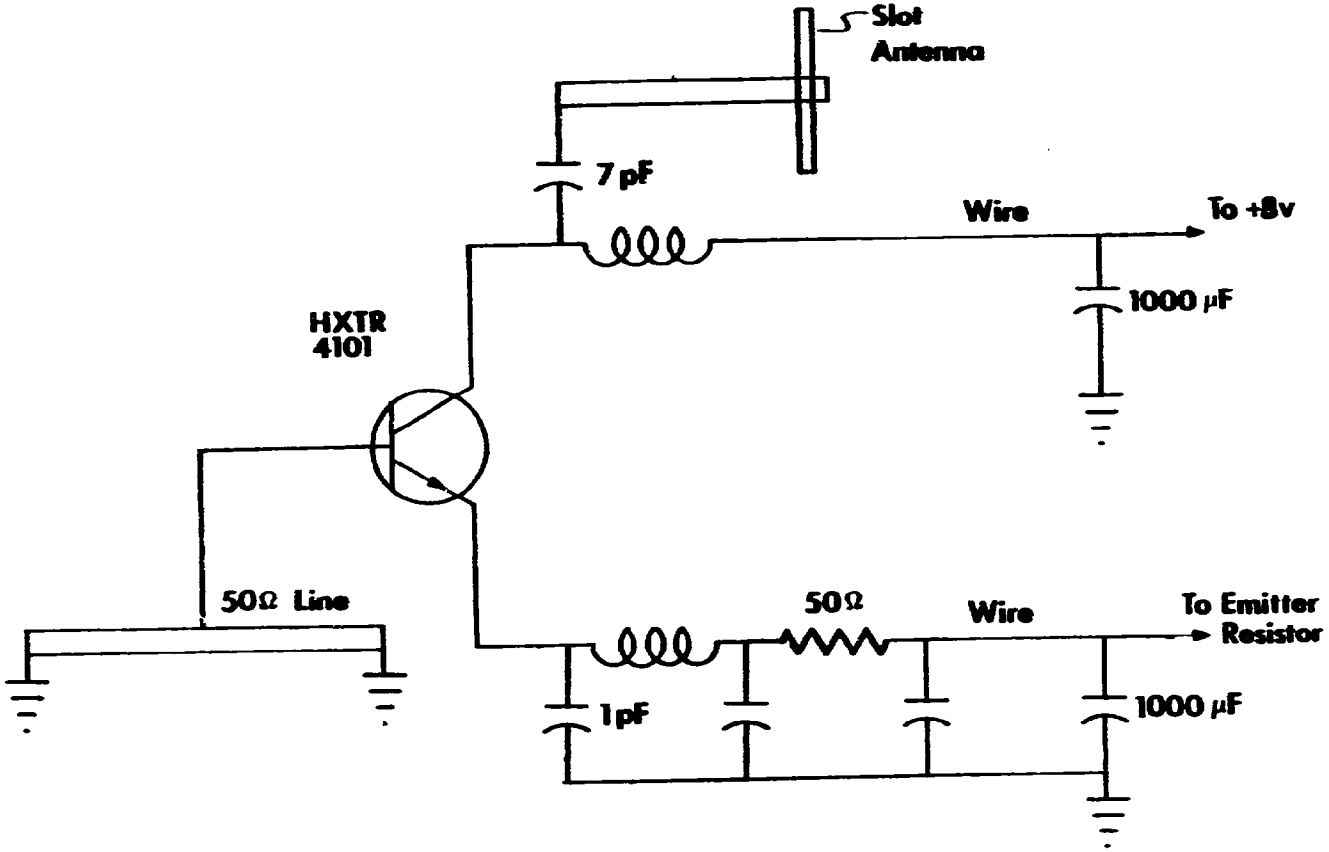

Figure 2. Motion Detection Sensor Schematic Diagram (5:13)

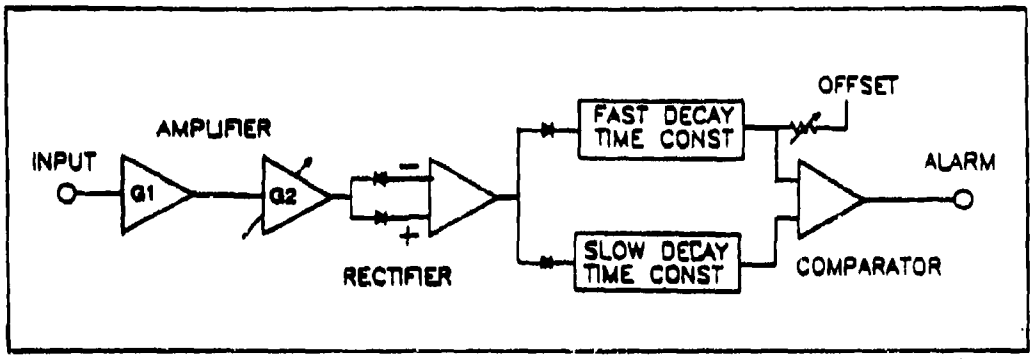

Figure 3. Block Diagram of Amplifier Processor Module (6:4)

eliminating most common-mode noise. Appropriate components are connected to the amplifier to provide interface to the motion detector sensor, dc voltage offset adjustment, variable gain, and a low pass filter. The first stage of the amplifier consists of three amplifiers. Gain (G1) of the first stage is not adjustable and is set at 785 by a 51Ω resistor. Gain G1 is given by Equation (1) as follows

$$G1 = 1 + 40K\Omega/51\Omega \qquad (1)$$

The second stage amplifier consists of a single amplifier and a resistor (R) variable from 0.0 to 100KΩ. Gain G2 is adjustable from 1.0 to 11 and is given by Equation (2) as

$$G2 = 110K\Omega/(R + 10K\Omega) \qquad (2)$$

Combined amplification of the two stages provides for an adjustable gain range of 785 to 8635 (29 to 39dB). In addition to amplification, the second stage amplifier also

performs low pass filtering. Cut off frequency (Fco) of the filter is given by Equation (3) and set at 3.1 Hz by a 0.47μF capacitor at the output of the amplifier.

$$Fco = 1/2\pi(110K\Omega)0.47\mu F \qquad (3)$$

Overall performance of the amplifier/filter circuit provides band-limited amplification of peak-input voltage signals from +/-0.9 to +/-10 mV.

Signal Processor Operation. The signal processor consists of a rectifier and a dual peak-detector comparator circuit. Their purpose is to convert output signals from the amplifier/filter from negative to positive polarity and provide a visual indication (via a LED) of the presence/absence of pulsatile motion at the surface of the motion detector sensor. Further information on the operation of these circuits can be obtained from references (5;6).

Arterial Pulse Monitor Modifications and Performance

Preliminary evaluations of the performance of the arterial pulse monitor were conducted on single subject using one pulse monitor. These evaluations were used to determine the pulse monitor modifications required to interface to the experimental setups for recording data. After completion of the modifications, additional performance evaluations were carried out using two of the modified pulse monitors. These additional performance

evaluations were accomplished to determine the optimum location for placement of the pair of pulse monitor sensors for recording data for subsequent use in developing test signals to evaluate the adaptive filter.

Arterial Pulse Monitor Modifications. Arterial pulse monitor modifications were evaluated using the pulse monitor evaluation setup. As previously stated, the pulse monitor evaluation setup was not a fixed design. Modifications occurred iteratively and were accomplished using the "test-a-little/evaluate/modify approach." Modifications were accomplished to establish electrical compatibility between the pulse monitor and the experimental setups used to record data. A summary of the modifications and the rationale for accomplishing them follows.

Sensor Mounting (Modification 1). The sensor mounting modification consisted of mounting a single arterial pulse monitor sensor inside each earpiece on a pair of headphones. This modification was accomplished to simulate a conformally fitted flight helmet recommended for pulse monitor sensor evaluation by Mawhinney (5:6) and to allow for easy relocation of the sensor to various areas in the temporal region for evaluation purposes.

Sensor Shielding (Modification 2). This second modification consisted of attaching a layer of ECCOSORB AN-P microwave absorbing foam to the side and back of each pulse monitor sensor. This modification was done to reduce the

effects of noise artifacts caused by background movement near the test subjects.

Signal Processor Module (Modification 3). The third modification removed the rectifier and the dual peak-detector comparator circuits from each pulse monitor amplifier/processor circuit board Figure (3). These circuits were removed because they added distortion and nonlinearities to the signals they processed and thus provided outputs incompatible for use in evaluating adaptive filter performance or accurate spectral analysis of pulse monitor signals.

Low Pass Filter (Modification 4). The low pass filter performed two functions in the experimental setups used in this thesis. These functions were noise removal and the prevention of signal aliasing during data sampling. The low pass filter modification consisted of replacing the pulse monitor's existing single-pole 3.1 Hz low pass filter with an eight-pole 9.0 Hz low pass filter. The modification involved removal of a 0.47μF capacitor from the output of second stage amplifier (Figure 3) and connecting amplifier's output to the input of the 9.0 Hz filter. The new output of the circuit was then obtained at the output of the 9.0 Hz filter. The 9.0 Hz low pass filter used was a Wavetek model 852 dual channel, eight-pole, high/low pass filter. The rationale for replacing the 3.1 Hz with the Wavetek filter was to utilize the Wavetek filter's switch selectable

capability for gains of 1.0 or 10 and cut-off frequencies from 0.1 Hz to 111 KHz. These switch selectable capabilities allowed rapid change in amplification levels and filter cut-off frequencies (and therefore sample rates), and thus minimized redesign down-time during experimental setup development. The 9.0 Hz cut-off frequency was selected as a trade-off between fast signal recovery time (after occurrence of large transient noise responses generated by the pulse monitor sensor) and minimizing the noise in the recorded data.

Amplifier Module (Modification 5). The amplifier module modification consisted of reducing the gain levels of the amplifiers on the pulse monitor's amplifier/processor circuit board and the using the amplification capability of the Wavetek model 852 high/low pass filter. The modification consisted of three steps. Step one involved replacement of a 51Ω resistor with a 1000Ω resistor in the first stage amplifier on the amplifier/processor circuit board (Figure 3). This change altered gain G1 from its previous value of 785 to a value of 41 where the altered gain G1 is given by Equation (4) as

$$G1 = 1 + 40K\Omega/1000\Omega \qquad (4)$$

Step two was accomplished by adjusting a 100KΩ variable resistor R in the second stage amplifier to produce amplifier gain G2 equal to 4.5. This new value of R was set

to approximately 14.4KΩ and was found by applying Equation (2). The final step of the modification was implemented simply by setting the gain switch on the Wavetek filter to 10x and leaving the filter installed at the output of second stage amplifier as previously discussed in the low pass filter modification. Total gain provided by the three step amplifier module modification was 1845. The rationale for selecting this gain value was to reduce the chance of pulse monitor output noise exceeding the +/-5v input level of Dash-16F A/D converter board and causing saturation of the board's amplifier and thus a nonrecoverable loss of signal in the recorded data. Rationale for reducing the gain in the first two stages of the pulse monitor amplifier and using the gain available from the low pass filter was to improve the output signal-to-noise ratio obtained by filtering some of the noise out prior to final amplification by the filter's amplifiers.

Arterial Pulse Monitor Performance. Performance characteristics of the arterial pulse monitor were evaluated using the ECG/pulse monitor setup and the pulse monitor evaluation setup (optimum configuration settings were used except as noted). Data collected from each setup was obtained from a single test subject with a different test subject used for each setup. Recorded data was evaluated in both the time and frequency domains. Remaining sections of this chapter will discuss the conditions under which the

performance evaluation data was obtained, the pulse monitor's signal and noise characteristics, and the selection of the optimum pulse monitor sensor position.

Performance Evaluation Conditions. The data used in the performance evaluation of the pulse monitor was obtained under the following conditions:

1. The pulse monitor and its sensor was used in a motion controlled environment which minimized extraneous noise artifacts.

2. The data was collected using the ECG/pulse monitor setup and the pulse monitor performance evaluation setup (optimum configuration used except as noted).

3. Data obtained from the test subject using the pulse monitor evaluation setup was collected from each of the four temporal regions defined in Figure 4.

4. Evaluation data obtained from the test subject using the EEG/pulse monitor setup was collected from temporal Region 3.

5. The type of noise data collected and evaluated was limited to noise caused by the types of facial muscular movement listed in the data sheets in Appendix A.

6. Heart rates of the test subjects did not exceed the range of 50 to 70 beats per minute.

Pulse Monitor Signal Characteristics. The pulse monitor is an extremely sensitive motion detector capable of detecting minute motion imperceptible to the unaided eye. Evaluation showed the monitor was capable of detecting pulsatile blood flow motion in superficially located arteries during the absence of muscular noise artifacts. Figures provided in Appendix B show some typical examples of the pulse signal waveforms and their respective power

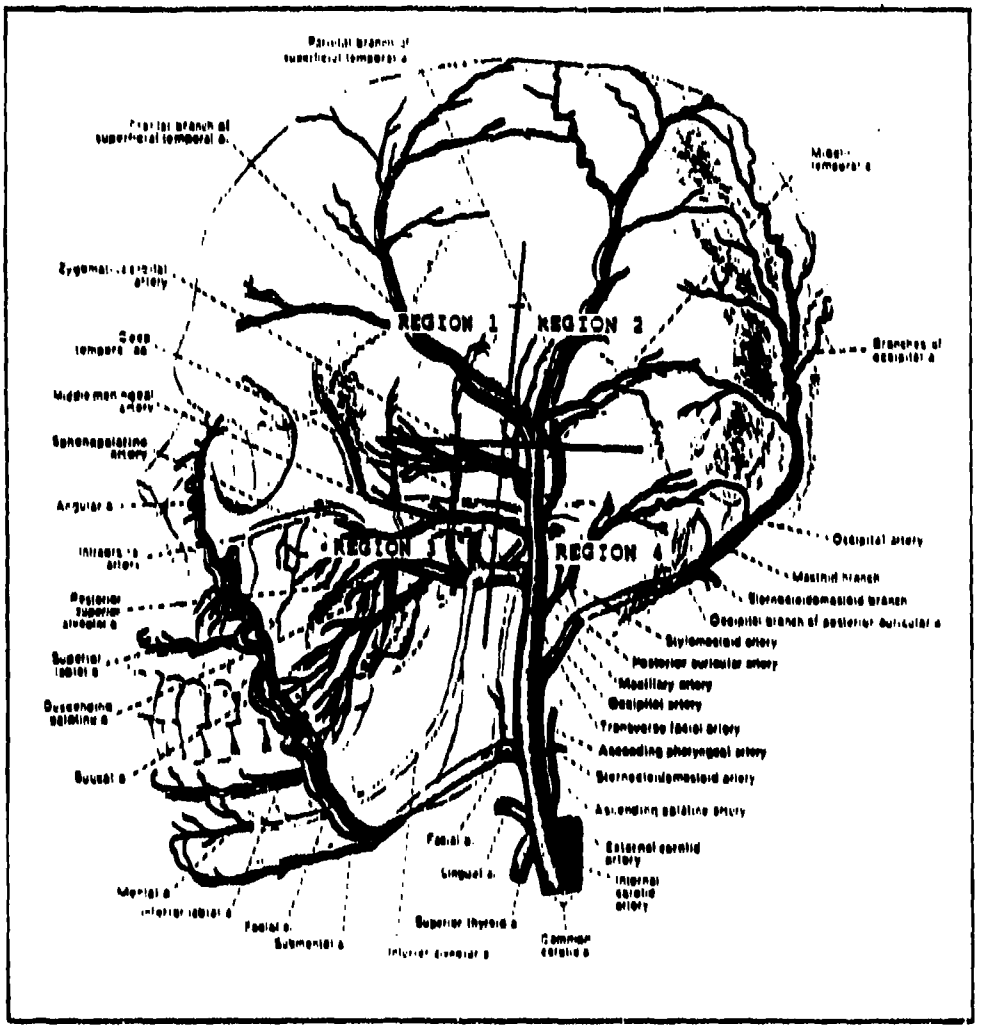

Figure 4. Temporal Evaluation Regions (4:618)

spectral densities for each of the four temporal regions evaluated. During evaluation, no distinct variations in pulse signal characteristics from region-to-region were observed other than peak signal amplitude values.

An important characteristic of the pulse monitor identified during its evaluation was its capability of

generating two distinct pulse signal outputs for any given single pulse. These two different pulse signal outputs can be identified by the polarity of their signal pulse peaks. Examples of these pulse types and their power spectral densities are given in Figures 5 and 6. This dual signal output characteristic of the pulse monitor is important because it can affect the level of success and the type of signal processing that can be accomplished on the pulse monitor's output. The output waveform characteristics in Figures 5 and 6 were observed in temporal Regions 1, 3 and 4; on both test subjects, using both single and multiple sensors. Generation of these two different types of pulse signal outputs were found to be independent of test subject, pulse monitor, amplifier configuration or sensor orientation. They were however found to be highly dependent upon sensor position; with changes as small as a millimeter determining whether the monitor's output was a positive or negative going pulse. The cause of this effect, although not fully understood, can probably be explained by tissue/bone movement in relation to the sensor (caused by pulsatile arterial motion) and the characteristic of the transducer to generate positive going signals when an object moves toward it and negative going signals when an object moves away. A power spectral density (1024 point FFT) of these two pulse signals in Figures 5 and 6 showed similar results with the largest spectral peak occurring at the test

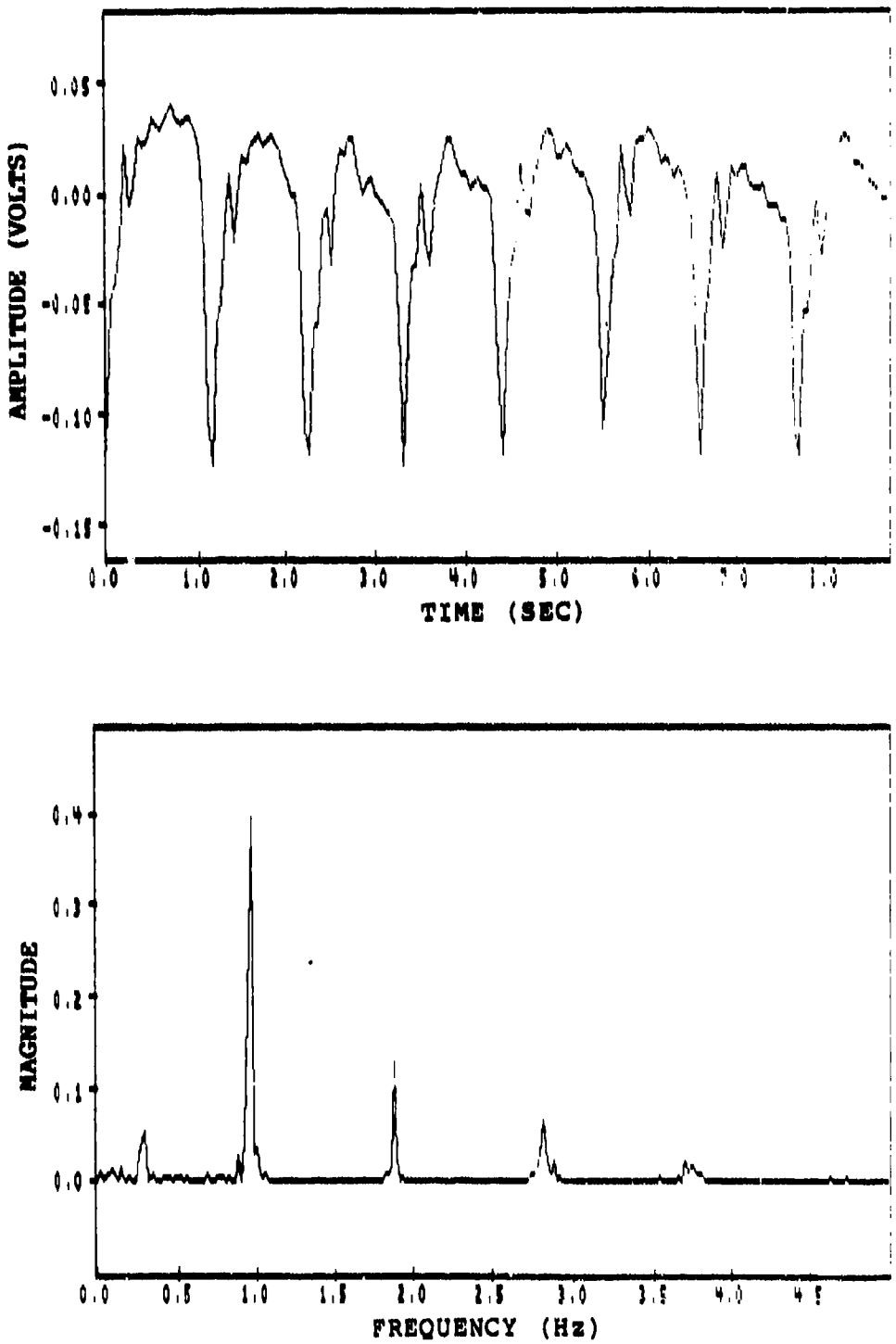

Figure 5. Region 3 Negative Pulse Signal (top) and its Power Spectral Density (bottom)

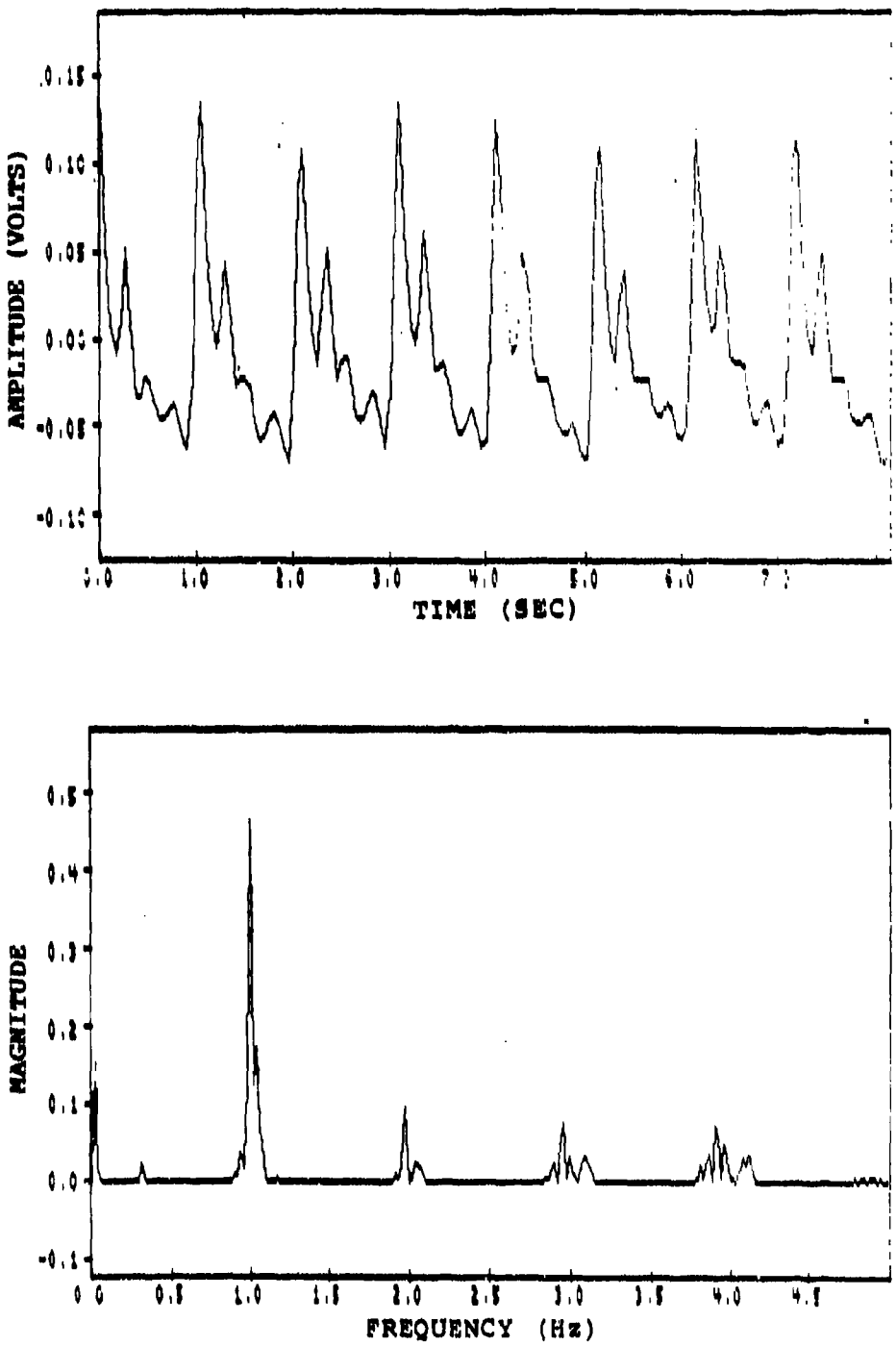

Figure 6. Region 3 Positive Pulse Signal (top) and its Power Spectral Density (bottom)

subject's heart rate frequency and additional spectral peaks of decreasing magnitude occurring at the higher harmonics. In addition, low magnitude spectral peaks were observed at frequencies below the test subject's heart rate frequency.

Another characteristic related to heart rate was the comparison of pulse monitor signal output with ECG data. This comparison of ECG data collected from one subject revealed a definite correlation between the occurrence of the ECG output and the output of the pulse monitor. A timing comparison of the ECG's E wave with the pulse monitor's signal peak showed a mean delay of 0.29 seconds for the test subject at a mean resting heart rate of 58.6 beats per minute.

In addition to the above, several regional differences in temporal characteristics were identified during the evaluation and are summarized by region as follows:

1) Region 1 pulse signals were difficult to acquire over most of the region using the pulse monitor. Once the sensor was properly positioned however, the pulse signals were characterized by fairly constant voltage levels. Signal levels ranged from no signal observed to peak values of approximately +/-0.2v. Region 1 was sensor orientation sensitive in some areas and provided peak signal output when the sensor's slot antenna was orientated perpendicular to the frontal branch of the superficial temporal artery (see Figure 4).

2) Region 2 pulse signals were very difficult to acquire and were characterized by inconsistent voltage levels over the entire region. Signal levels ranged from no signal observed to peak values of approximately +0.06v. Signal levels were very difficult to maintain and were frequently lost due to slight movements of the pulse monitor. Region 2 was sensor orientation sensitive and the only signals obtained were when the sensor's slot antenna was orientated perpendicular to the parietal branch of the superficial temporal artery.

3) Region 3 pulse signals were fairly easy to acquire and were characterized by fairly constant voltage levels when the sensor was placed in the center of region. Signal levels ranged from no signal observed to peak values of approximately +/-0.4v. Pulse signals were almost continuously available in the center of Region 3, but most of these signals were low level and a certain degree of sensor repositioning was required to obtain a strong signal (greater than +/-0.2v). Once acquired however, signal levels could be maintained at a fairly constant level even after a slight movement of the pulse monitor. Region 3 exhibited a strong tendency to generate the dual signal polarity characteristic previously identified. Region 3 was not sensor orientation sensitive and strong signals were obtained for horizontal, vertical and diagonal sensor orientations.

4) Region 4 pulse signals were easy to acquire and were characterized by strong but variable voltage levels. Data collection runs typically had peak voltage variations as high as 0.2v due to positional changes of the sensor caused by muscular movement. Pulse signals were available over most of the region and ranged from no signal observed to +/-0.6v. Region 4 exhibited a strong tendency to generate the dual signal polarity characteristic previously identified. The region was somewhat sensor orientation sensitive with the strongest signals obtained with the sensor's slot antenna oriented horizontal to the ground and weaker (but still strong) signals obtained with a vertical sensor orientation.

Pulse Monitor Noise Characteristics. The pulse monitor is extremely susceptible to motion caused by muscular movement. Evaluation was limited to noise caused by the types of facial muscular movements listed in the two data collection sheets contained in Appendix A. These types of movements were selected to provide a good representative collection of noise artifacts generated by the pulse monitor and used for investigating the feasibility of using an adaptive filter for noise reduction of pulse monitor noise artifacts.

Figures provided in Appendix C show a complete example of a noise correlation data run recorded with two pulse monitors. The pulse monitor sensors were mounted on the

left and right temporal Region 3 of the test subject with the amplifier gains set at 184.5. Each figure provides a comparison of noise data recorded simultaneously from each of the sensors.

Figures provided in Appendix D show a complete single channel example of a sensor test data run (signal-plus-noise) recorded from a pulse monitor. The data displayed was collected from the right temporal Region 3 of a test subject. The first figure shows a 9.0 second example of a negative going pulse signal during the absence of muscular movement. Peak amplitude of the pulse signal is approximately -0.12v. Subsequent figures show the same type of pulse signal from the first figure recorded during various types of muscular movement. These figures are provided as a representative sampling of signal-plus-noise data and are included here to provide a comparison between the signal and various levels of noise obtained with the pulse monitor.

Evaluation of the pulse monitor in the temporal region showed muscular movement generated noise artifacts that were transient and nonperiodic in nature. Noise artifacts caused by different muscular movements had little similarity (in frequency and amplitude content) from artifact-to-artifact and appeared to exhibit nonstationary characteristics. Comparison of dual sensor noise data (recorded simultaneously) showed changes in noise correlation between

sensors, with variations observed in both frequency and amplitude content. Touching or moving the sensor with an external force when it was attached to a test subject was observed to almost always cause amplifier saturation (+/-5v). Signal-to-noise levels as low as -14 dB were routinely observed during muscular movement even when strong pulse signals (+/-0.2v) were present. Muscular movement was frequently observed to cause repositioning of the sensor, reduction/loss of signal and generation of large noise artifacts. Since the position of the sensor was always optimized for maximum pulse signal output for each area under study, movement of the sensor almost always caused a reduction or loss of the pulse signal voltage level. The largest noise levels observed for muscular movements were caused by moving the jaw; while face flexing and eye movements were found to produce very little noise artifact.

Sensor-to-sensor comparison of the noise data varied widely from good correlation to no correlation observed (the word correlation as used in this section is subjective and was based on the visual comparison of two-channel data for similarities in their waveforms). Correlation was highly dependent on sensor location and the type of noise monitored. The best correlation was obtained for jaw movements such as opening and closing the mouth, and biting/gritting the teeth. Eye movements and face flexing produced some of the worst correlation. Speaking, yawning

and swallowing were characterized by random correlation, with some movements producing good correlation while others showing little or none. Fluctuations between negative and positive correlation were frequently observed for similar jaw movements in Regions 3 and 4. This correlation fluctuation appeared similar in characteristics to those observed for the dual polarity pulse signals and could, as a result, possibly be related in its cause.

Overall, results of the noise evaluation agree with previous results obtained by Mawhinney (5) where output waveforms between multiple sensors were variable and lacked similarity "even when the sensors were exposed to similar artifact motion" (5:4-5).

Pulse Monitor Sensor Placement. During preliminary evaluation of the pulse monitor, the pulse monitor's sensor was moved to multiple locations in the temporal region of the test subject to determine the optimum location to record evaluation data. During this portion of the evaluation, it was discovered that different areas of the temporal region produced different amplitudes of pulse signals and varying degrees of difficulty in acquiring and maintaining pulse signals amplitudes. Based on this observation, the temporal area of the test subject was divided into four loosely defined regions and numbered 1 through 4 as shown in Figure 4. Regional dividing lines were approximate with some degree of overlap of the regional

characteristics in the transitional zones between the regions.

Selection of the optimum location to record evaluation data was subjective and was based solely on pulse signal characteristics. Region 3 was selected as the optimum data recording location because results of pulse signal evaluation showed the region had the best all around signal characteristics; with ease of acquisition, strong signals and fairly constant signal levels.

IV. Test Signal Development

Introduction

Previous chapters have covered background information, discussed experimental data collection and evaluation of the arterial pulse monitor. This chapter will continue with a description of the development of the test signals which were used to evaluate the feasibility of using a LMS adaptive filter with the arterial pulse monitor.

Test signals were constructed in pairs and consisted of a signal-plus-noise test signal and a noise test signal. The noises in each test signal were correlated and a total of three different pairs of test signals were developed.

The remaining portions of this chapter are organized into development of the arterial pulse signal, the correlated noise signal pair and the test signal pair.

Arterial Pulse Signal Development

The arterial pulse test signal was developed from an ensemble average of 112 seconds of a negative going arterial pulse signal recorded from temporal Region 3. The ensemble average of this signal was constructed by separating the signal into 122 individual peak-to-peak signal segments of various lengths. These 122 segments were further separated by signal lengths into 5 groups ranging in length from 20 to 24 data points. The average signal length of the ensemble average was chosen as 22 data points and was based on the

largest number of peak-to-peak segments (43) of the same length from among the total number of signal segments. The ensemble average of these 43 signal segments was then completed and a single period of an arterial pulse test signal was obtained.

The final arterial pulse test signal was obtained by replicating the single period of test signal 109 times to produce a test signal 120 seconds long. Figure 7 shows a 9.0 second representative sample of the ensemble averaged arterial pulse test signal. This test signal represents a pulse rate of approximately 54 beats per minute. For a comparison with an actual Region 3 pulse signal see Appendix D, Figure 31.

Correlated Noise Signal Pair Development

Three correlated noise test signal pairs were developed by using noise outputs from a pair of pulse monitor sensors mounted on a test subject's left and right temporal Region 3. These three test signal pairs are shown in Appendix C, Figures 26, 27 and 28. These signals were chosen because they provided good representations of three types of correlation (positive, negative and intermittent) obtained from the arterial pulse monitor. Development of these signals consisted of adding 6.0 seconds of straight line (0.0v) data on the end of each signal to provide a small sample of signal only data to compare with the signal output of the adaptive filter.

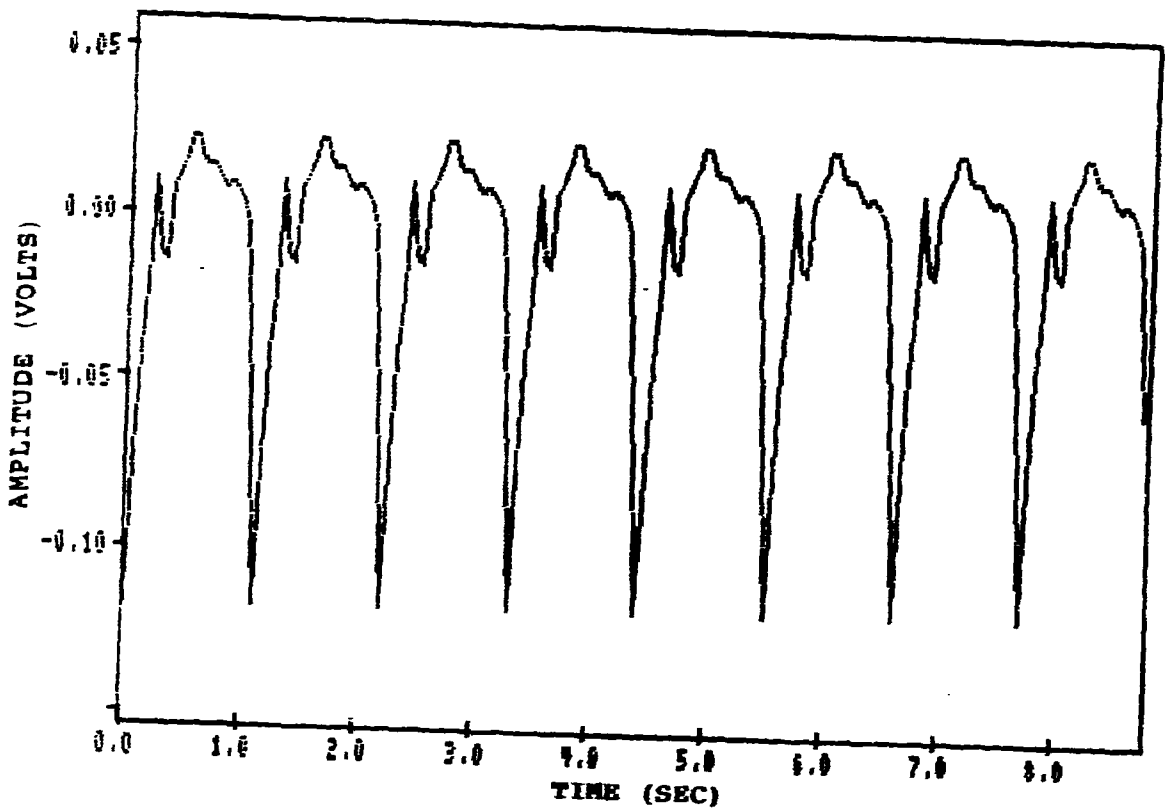

Figure 7. Ensemble Averaged Arterial Pulse Test Signal

Test Signal Pair Development

The test signal pairs were the signals used in the evaluation of the adaptive filter. These signal pairs are shown in Figures 8, 9 and 10; and were developed using the arterial pulse test signal and the correlated noise test signal pairs. Development of these signals consisted of adding the arterial pulse test signal, cut to an appropriate length of time, to a single noise signal contained in one of the correlated noise test signal pairs. The remaining noise signal in the correlated noise test signal pair was then left unmodified. The results of this provided a test signal pair containing a signal-plus-noise test signal and a correlated noise test signal.

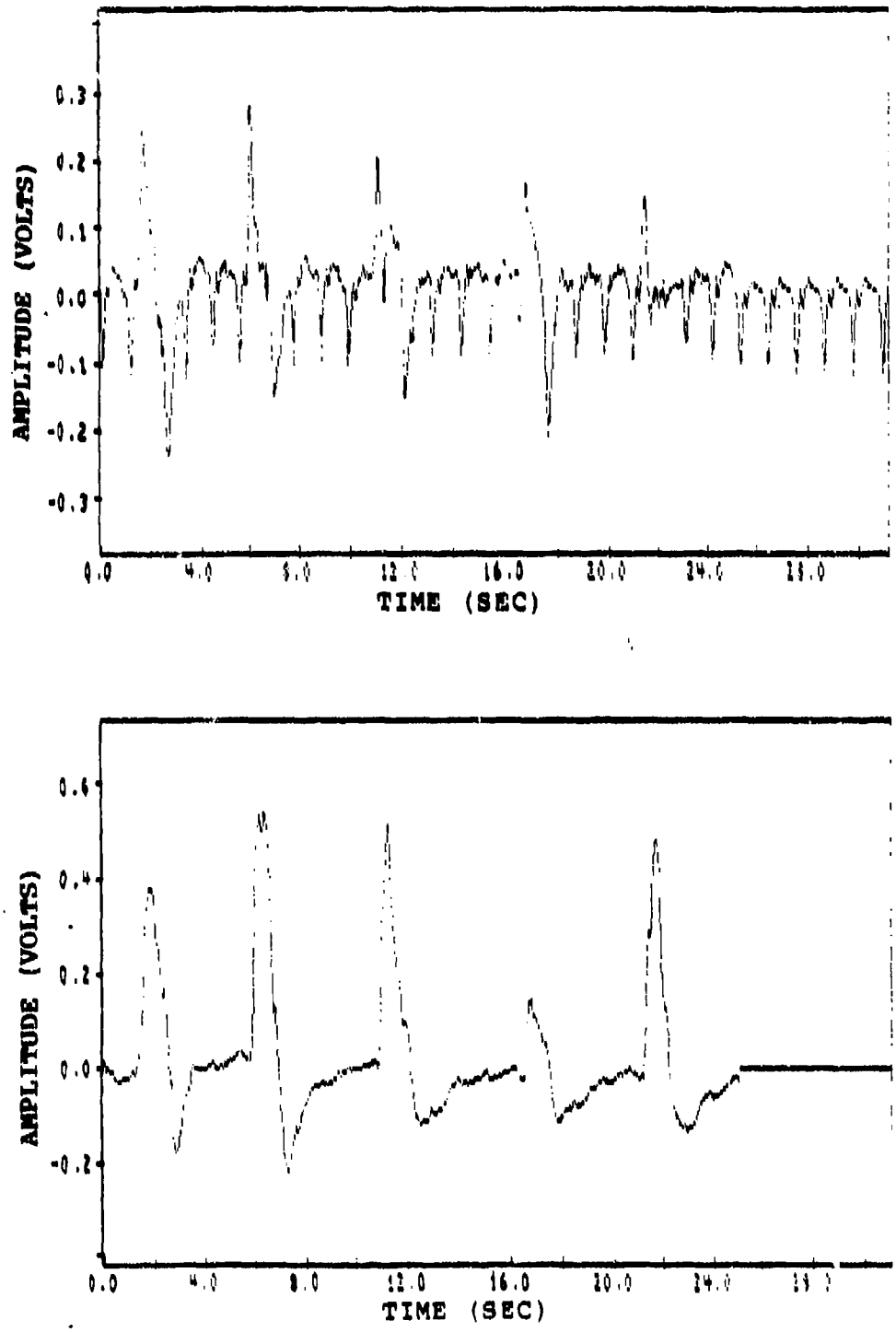

Figure 8. Positive Correlation Test Signal Pair, Signal-Plus-Noise (top), Noise (bottom)

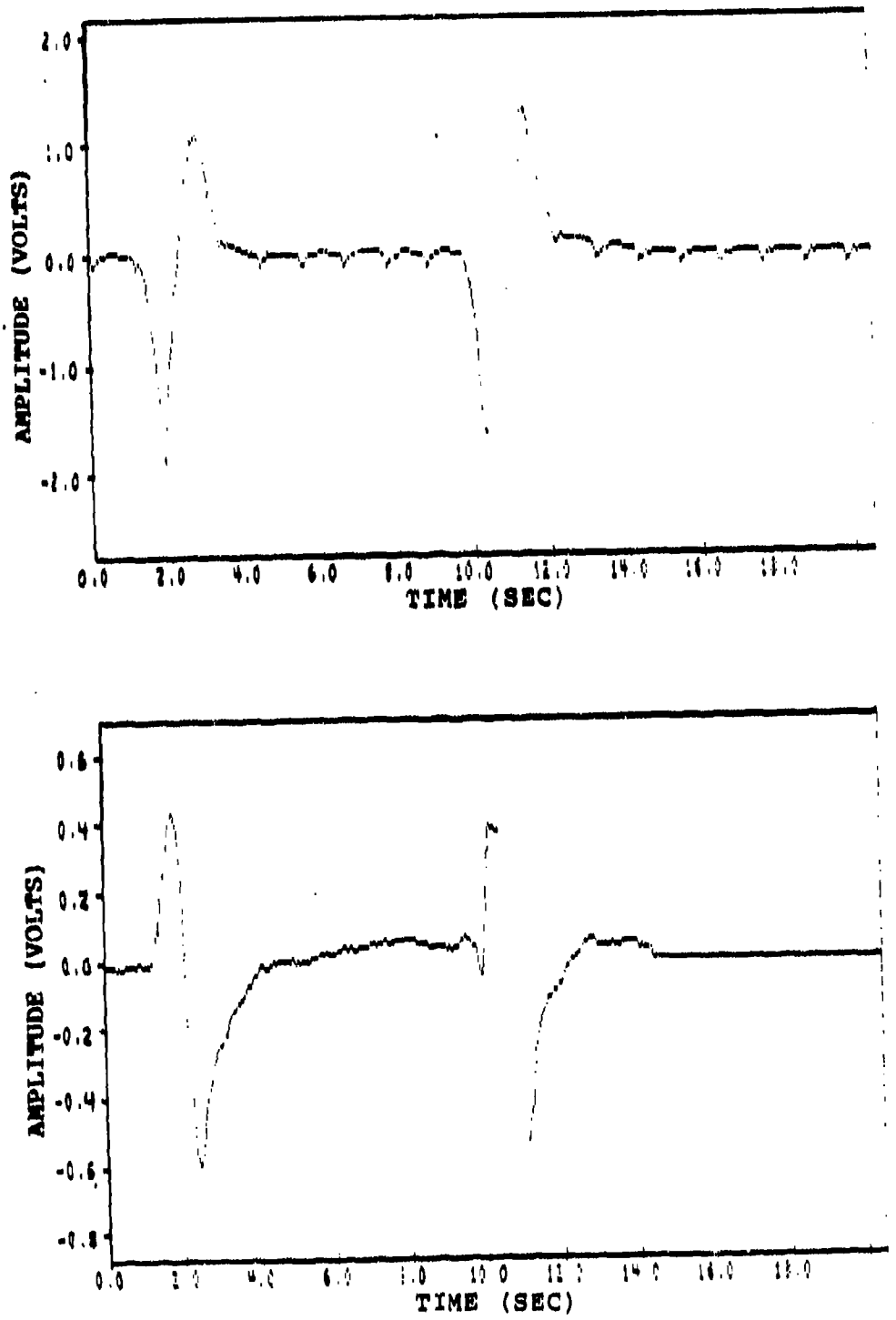

Figure 9. Negative Correlation Test Signal Pair, Signal-Plus-Noise (top), Noise (bottom)

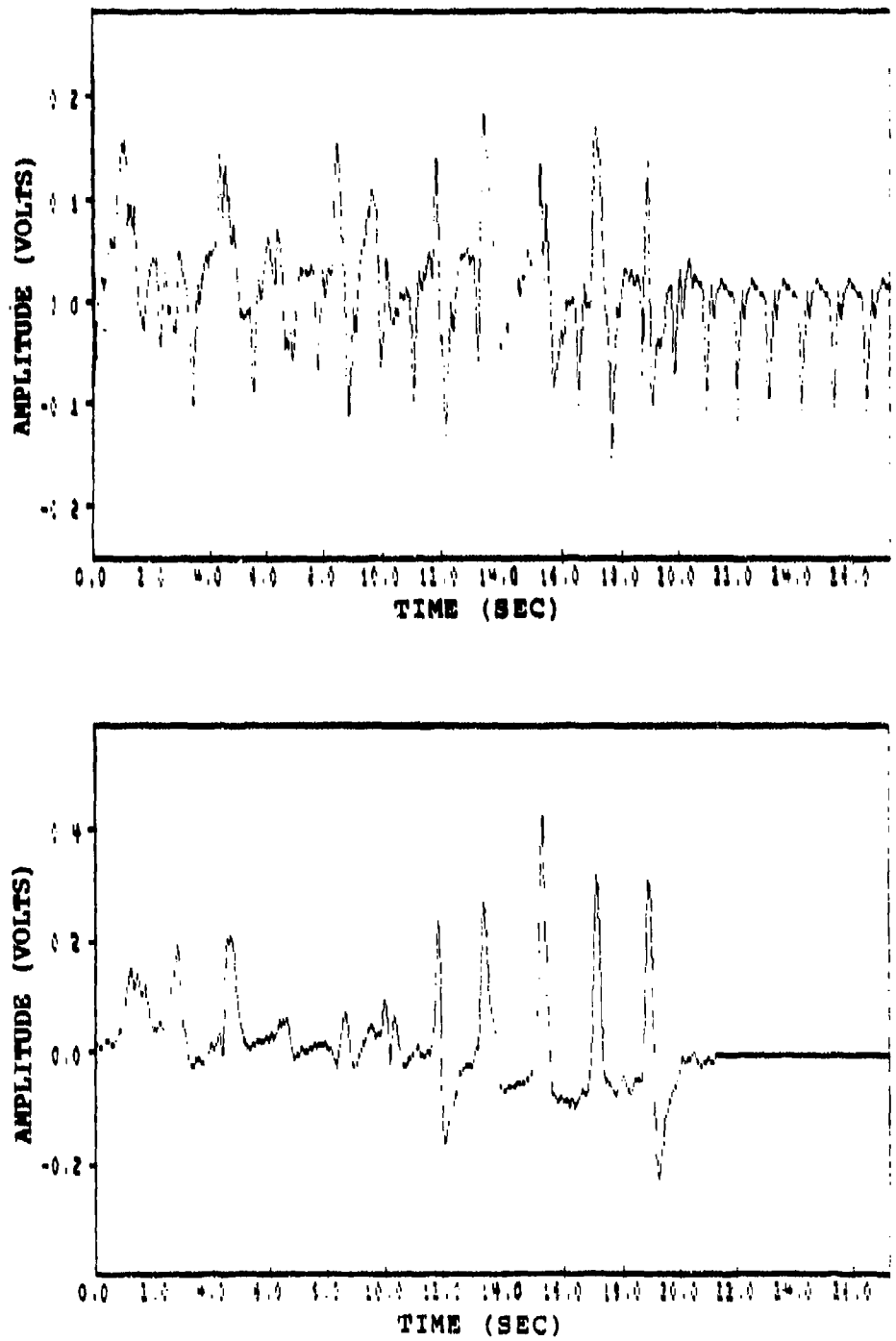

Figure 10. Intermittent Correlation Test Signal Pair, Signal-Plus-Noise (top), Noise (bottom)

V. LMS Adaptive Noise Cancellation Filter

Introduction

Previous chapters have evaluated the performance of the arterial pulse monitor and developed a set of test signals from recorded pulse monitor data. This chapter will apply these results and determine the feasibility of using a LMS adaptive filter with the arterial pulse monitor. The following sections of this chapter will discuss LMS adaptive filter theory, software implementation of the filter and finally, results of the experimental evaluation of the filter using the test signal data developed in Chapter 4.

LMS Adaptive Filter Theory (1;15;16;17;18)

Signal recovery from noisy channels has traditionally been accomplished using filters. Filters normally operate by amplifying a desired signal while suppressing unwanted noise. Filters can be classified as either fixed or adaptive.

Fixed filters are usually used in cases where the desired signal is contained within a fixed bandwidth and the noise frequency spectrum lies outside this bandwidth. Design of fixed filters requires prior knowledge of both signal and noise characteristics.

Adaptive filters however, are usually used when the signal or noise characteristics are variable over time or unknown. Adaptive filters are self adjusting and can have

the capability of tracking and recovering signals that are nonstationary. Use of an adaptive filter normally requires inputs from multiple sources as shown in Figure 11. For an

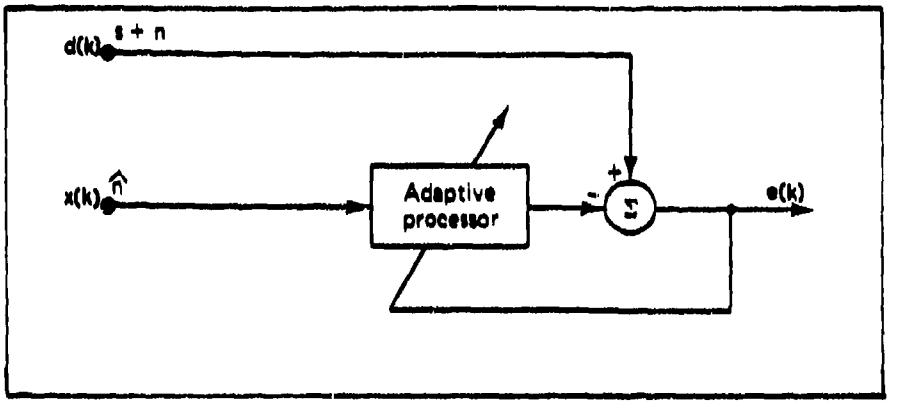

Figure 11. Adaptive Noise Cancellation Filter (15:10)

adaptive noise cancellation filter, the required inputs consist of a signal-plus-noise input d(k) and a reference noise input x(k). The signal-plus-noise input d(k) contains a signal s and a noise n. Noise n is uncorrelated with signal s. The reference noise input x(k) contains a noise $\hat{n}$. This noise $\hat{n}$ is uncorrelated with signal s and correlated with noise n in some unknown way.

Operation of the adaptive noise cancellation filter consists of filtering $\hat{n}$ with the adaptive processor to produce an output $\tilde{n}$ that is similar to n. The output of the adaptive processor is then subtracted from the input d(k) and a system output $e(k) = s + n - \tilde{n}$ is obtained. Adaptation of the filter is accomplished by feedback of the e(k) signal to the adaptive processor where the filter

parameters are updated. The entire process then repeats itself and a new e(k) is produced. Eventually, the adaptive processor converges (adapts) to an optimum condition and produces an output that approaches n such that, the difference between n and $\hat{n}$ is minimized and $e(k) \simeq s$.

The performance of the adaptive processor depends on many conditions such as: the filter algorithm used, the input signal characteristics and the filter parameters. The next section of this thesis will discuss these conditions and how they affect the performance of the LMS adaptive noise cancellation filter.

LMS Adaptive Filter Algorithm. The LMS adaptive filter algorithm can be implemented using the filter in Figure 12.

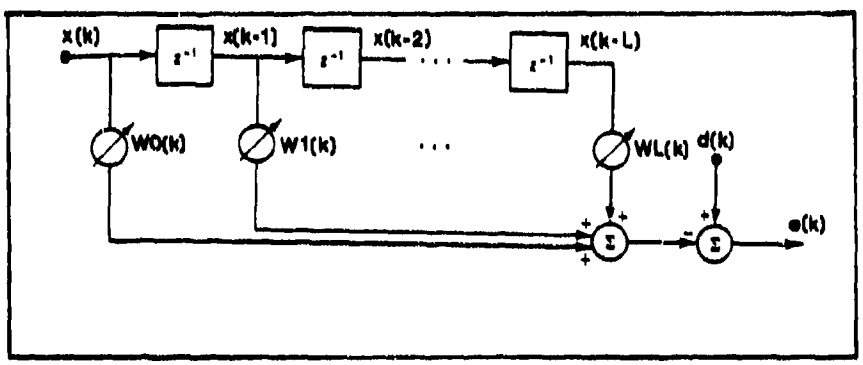

Figure 12. Adaptive Linear Combiner Transversal Filter (15:101)

Output of this filter is defined by (15:100) as

$$e(k) = d(k) - \underline{X}^T(k)\underline{W}(k) \qquad (5)$$

where

$e(k)$ = scaler signal output of filter at time k
$d(k)$ = scaler signal-plus-noise input of filter at time k
T = transpose
$\underline{X}(k)$ = correlated reference noise input vector of filter at time k
$= [x(k), x(k-1), x(k-2), \ldots, x(k-L)]^T$
$\underline{W}(k)$ = filter weight vector at time k
$= [W0(k), W1(k), W2(k), \ldots, WL(k)]^T$
L = filter order

Operation of the LMS adaptive noise cancelation filter consists of adjusting the weights to an optimum weight vector solution where the noise at output $e(k)$ of the filter is minimized. This optimum weight vector solution is obtained when the product of the filter's reference noise input vector $\underline{X}(k)$ and its weight vector $\underline{W}(k)$ is approximately equal to the noise component of the signal-plus-noise input $d(k)$ of the filter. For the LMS filter, the weight adjustment uses an algorithm derived from the gradient estimate $\hat{\nabla}(k)$ of the filter's output power $e^2(k)$ with respect to the weight vector $\underline{W}(k)$ at each iteration in the adaptive process. This gradient estimate $\hat{\nabla}(k)$ is defined by Widrow (15:100) as

$$\hat{\nabla}(k) = -2e(k)\underline{X}(k) \tag{6}$$

After applying this definition to the steepest descent algorithm (15:57)

$$\underline{W}(k+1) = \underline{W}(k) - \mu\hat{\nabla}(k) \tag{7}$$

the Widrow-Hoff LMS algorithm (18:1708) is obtained and is given by

$$\underline{W}(k+1) = \underline{W}(k) + 2\mu e(k)\underline{X}(k) \tag{8}$$

where μ is the convergence parameter that controls the speed, noise and the stability of the adaptation.

By assuming $d(k)$ and $\underline{X}(k)$ are stationary stochastic processes with $\underline{W}(k)$ independent of $\underline{X}(k)$ and μ adjusted for convergence. The LMS algorithm adaptation and convergence to the optimum weight vector $\underline{W}^*$ can be determined by taking the expected value of both sides of Equation (8) as follows

$$E\{\underline{W}(k+1)\} = E\{\underline{W}(k)\} + 2\mu E\{e(k)\underline{X}(k)\} \tag{9}$$

By assuming convergence, after a sufficient number of iterations, $E\{\underline{W}(k+1)\}$ and $E\{\underline{W}(k)\}$ will approach to roughly the same values and be approximately equal to the optimum weight vector $\underline{W}^*$. Using these results, Equation (9) can then be approximated by

$$E\{e(k)\underline{X}(k)\} = \underline{0} \tag{10}$$

This result can be verified by noting the same result would have been obtained by taking the expected value of Equation (6) and fixing the weight vector at its optimum solution where $E\{\hat{\nabla}(k)\} = \underline{0}$. Continuing with Equation (10), substitute in Equation (5) for $e(k)$ to obtain

$$E\{d(k)\underline{X}(k) - \underline{X}^T(k)\underline{W}(k)\underline{X}(k)\} = \underline{0} \tag{11}$$

where after rearranging the terms and substituting $\underline{W}^*$ for $E\{\underline{W}(k)\}$

$$E\{d(k)\underline{X}(k)\} - E\{\underline{X}(k)\underline{X}^T(k)\}\underline{W}^* = \underline{0} \tag{12}$$

By using the following definitions, where the cross correlation vector between the signal-plus-noise input and the correlated reference noise input is given by

$$E\{d(k)\underline{X}(k)\} = \underline{P} \tag{13}$$

and the signal-plus-noise autocorrelation matrix is given by

$$E\{\underline{X}(k)\underline{X}^T(k)\} = \underline{R} \tag{14}$$

Equation (12) can be rewritten as

$$\underline{P} - \underline{R}\underline{W}^* = \underline{0} \tag{15}$$

and the optimum weight vector $\underline{W}^*$ solution for the LMS adaptive noise cancellation filter can be calculated (assuming $\underline{R}$ is invertible) as

$$\underline{W}^* = \underline{R}^{-1}\underline{P} \tag{16}$$

Using this result for the optimum weight vector solution, it is now possible to investigate the effects of input noise characteristics on the performance of the LMS adaptive noise cancellation filter. Two classes of signal input noise data will be investigated, nonstationary noise and uncorrelated noise.

LMS Performance with Nonstationary Noise Inputs.

Nonstationary noise inputs to the LMS adaptive noise cancellation filter can seriously affect the performance of the filter depending on the degree of nonstationarity exhibited. To simplify the following performance analysis, the nonstationary noise is assumed to be correlated and contained in both filter inputs d(k) and x(k). The effects of this nonstationary noise can be readily seen by examining the optimum weight vector solution given by Equation (16) and the correlation Equations (13) and (14). For nonstationary input signals d(k) and x(k), $\underline{P}$ and $\underline{R}$ will vary with respect to time and cause the optimum weight vector solution $\underline{W}^*$ to change constantly. This constant change will force the filter weight vector $\underline{W}(k)$ to continually adapt in an attempt to track the optimum weight vector solution which minimizes the filter output noise. Depending on the severity of the nonstationarity, the filter may or may not be able to successfully track the optimum weight vector solution to produce a filter output with a satisfactory signal-to-noise ratio. This effect can be seen by rearranging Equation (8) as follows

$$\underline{W}(k+1) - \underline{W}(k) = 2\mu e(k)\underline{X}(k) \tag{17}$$

and taking the expected value of both sides

$$E\{\underline{W}(k+1) - \underline{W}(k)\} = 2\mu E\{e(k)\underline{X}(k)\} \tag{18}$$

After a sufficient number of iterations $\underline{W}(k)$ approaches the optimum weight vector $\underline{W}^*$ and $\underline{W}(k+1)$ approaches a weight vector value $\underline{W}$ which lags behind $\underline{W}^*$ and is dependent upon the degree of input noise nonstationarity. These results yield the following expression

$$E\{\underline{W} - \underline{W}^*\} = 2\mu E\{e(k)\underline{X}(k)\} \tag{19}$$

The difference between these two weight vectors can be defined as a weight deviation vector $\underline{V}$ where

$$\underline{V} = \underline{W} - \underline{W}^* \tag{20}$$

Upon substituting this result in Equation in Equation (19)

$$E\{\underline{V}\} = 2\ E\{e(k)\underline{X}(k)\} \tag{21}$$

and performing the following derivations

$$E\{\underline{V}\} = 2\mu E\{d(k)\underline{X}(k) - \underline{X}^T(k)\underline{W}(k)\underline{X}(k)\} \tag{22}$$

$$E\{\underline{V}\} = 2\mu E\{d(k)\underline{X}(k) - \underline{X}(k)\underline{X}^T(k)\underline{W}(k)\} \tag{23}$$

$$E\{\underline{V}\} = 2\mu(\underline{P} - \underline{R}\underline{W}) \tag{24}$$

a result for the mean weight deviation vector is obtained which is dependent upon the degree of noise nonstationarity in the input noise (the crosscorrelation vector and the autocorrelation matrix) to the adaptive filter.

For an example where successful tracking may not be possible is for transient random noise, where irregular

changes of the optimum weight vector solution may prevent the filter from adapting fast enough (thereby increasing the size of the weight deviation vector $\underline{V}$) to successfully reduce the noise in the filter's output. In a case such as this, filter performance may be erratic, with unacceptable output noise as the filter's weights continually adapt and readapt from transient-to-transient in an attempt to minimize the output noise.

LMS Performance with Uncorrelated Noise Inputs.

Uncorrelated noise inputs to the LMS adaptive noise cancellation filter can cause degraded performance by increasing the filter's output noise level. For the purpose of this performance analysis, correlated noise inputs n(k) and $\hat{n}$(k) are applied respectively to both d(k) and x(k) of the adaptive filter and an uncorrelated noise input n'(k) is applied to either the d(k) or x(k) input. The effects of an uncorrelated noise on the performance results obtained at the filter's output can be investigated by examining Equations (5), (13), (14) and (16). By using Equation (5), the adaptive filter's output e(k) is shown to be a function of the noise applied to input d(k), minus a filtered version of the noise applied to input x(k).

For the case of correlated noise applied to both inputs of the adaptive filter, the filter's weight vector $\underline{W}$(k) converges to the optimum solution $\underline{W}^*$ given by Equation (16).

With $\underline{X}(k) = \underline{N}(k)$ and $d(k) = n(k)$ the crosscorrelation vector $\underline{P}$ is given by

$$\underline{P} = E\{n(k)\underline{N}(k)\} \tag{25}$$

and the autocorrelation matrix $\underline{R}$ is given by

$$\underline{R} = E\{\underline{N}(k)\underline{N}^T(k)\} \tag{26}$$

Using these results, Equation (16) for the optimum weight vector solution $\underline{W}^*$ for correlated noise inputs can then be rewritten as

$$\underline{W}^* = E\{\underline{N}(k)\underline{N}^T(k)\}^{-1} E\{n(k)\underline{N}(k)\} \tag{27}$$

When this $\underline{W}^*$ is used to filter input $x(k)$, an output is produced which is similar to $d(k)$. Using this result with Equation (5), the output of the adaptive filter can be calculated and will contain a minimum of noise and be approximately equal to zero.

For uncorrelated noise, the adaptive filter's performance varies depending upon where this noise is applied to the filter.

When the uncorrelated noise is applied to the $d(k)$ input of the filter, $d(k) = n(k) + n'(k)$; the $\underline{R}$ matrix remains unchanged and the $\underline{P}$ vector is redefined as

$$\underline{P} = E\{[n(k) + n'(k)]\underline{N}(k)\} \tag{28}$$

After multiplying terms

$$\underline{P} = E\{n(k)\underline{N}(k) + n'(k)\underline{N}(k)\} \tag{29}$$

and then rearranging them, it follows that

$$\underline{P} = E\{n(k)\underline{N}(k)\} + E\{n'(k)\underline{N}(k)\} \tag{30}$$

Since $n'(k)$ is uncorrelated with $\underline{N}(k)$, $E\{n'(k)\underline{N}(k)\} = \underline{0}$ and the crosscorrelation vector $\underline{P}$ becomes

$$\underline{P} = E\{n(k)\underline{N}(k)\} \tag{31}$$

This result is the same as obtained for the correlated input noise case and therefore the optimum weight vector solution is identical in value as that obtained for the correlated noise case previously described. This optimum weight vector therefore greatly reduces or eliminates the correlated noise inputs from the adaptive filter's output $e(k)$. Since by Equation (5), the optimum weight vector solution does not directly act upon the $d(k)$ input, $d(k) = n(k) + n'(k)$, the uncorrelated noise is left unchanged and appears directly in the output of filter. Depending upon the strength of this uncorrelated noise, this noise may or may not significantly impact the performance of the adaptive filter.

For the case when uncorrelated noise is applied to the $x(k)$ input of the filter, $\underline{X}(k) = \underline{N}(k) + \underline{N}'(k)$; the $\underline{P}$ vector and the $\underline{R}$ matrix are redefined as follows

$$\underline{P} = E\{n(k)[\underline{N}(k) + \underline{N}'(k)]\} \tag{32}$$

$$\underline{R} = E\{[\underline{N}(k) + \underline{N}'(k)][\underline{N}(k) + \underline{N}'(k)]^T\} \quad (33)$$

For the $\underline{P}$ vector, upon multiplying terms

$$\underline{P} = E\{n(k)\underline{N}(k) + n(k)\underline{N}'(k)\} \quad (34)$$

and then rearranging them, it follows that

$$\underline{P} = E\{n(k)\underline{N}(k)\} + E\{n(k)\underline{N}'(k)\} \quad (35)$$

Since $n(k)$ is uncorrelated with $\underline{N}'(k)$, $E\{n(k)\underline{N}'(k)\} = \underline{0}$ and the crosscorrelation vector $\underline{P}$ becomes

$$\underline{P} = E\{n(k)\underline{N}(k)\} \quad (36)$$

This vector is the same as that obtained for the correlated and uncorrelated noise cases previously described and therefore has no affect on the change in the optimum weight vector solution. For the case of the $\underline{R}$ matrix, after multiplying terms in Equation (33)

$$\underline{R} = E\{\underline{N}(k)\underline{N}^T(k) + 2\underline{N}(k)\underline{N}'^T(k) + \underline{N}'(k)\underline{N}'^T(k)\} \quad (37)$$

and upon rearranging them, it follows that

$$\underline{R} = E\{\underline{N}(k)\underline{N}^T(k)\} + 2E\{\underline{N}(k)\underline{N}'^T(k)\} + E\{\underline{N}'(k)\underline{N}'^T(k)\} \quad (38)$$

Since $\underline{N}(k)$ is uncorrelated with $\underline{N}'(k)$, $E\{\underline{N}(k)\underline{N}'^T(k)\} = \underline{0}$ and the autocorrelation matrix $\underline{R}$ becomes

$$\underline{R} = E\{\underline{N}(k)\underline{N}^T(k)\} + E\{\underline{N}'(k)\underline{N}'^T(k)\} \quad (39)$$

This result for the $\underline{R}$ matrix is unlike the previous cases observed and contains an additional term for the autocorrelation of the uncorrelated noise. This new term completely changes the $\underline{R}$ matrix and as a result, a new optimum weight vector solution is produced which is given as follows

$$\underline{W} = [E\{\underline{N}(k)\underline{N}^T(k)\} + E\{\underline{N}'(k)\underline{N}'^T(k)\}]^{-1} E\{n(k)\underline{N}(k)\} \quad (40)$$

This new optimum weight vector solution has performance characteristics which eliminates the uncorrelated noise from the x(k) input and produces an output which closely resembles the noise input at d(k). By using this result with Equation (5), the adaptive filter output o(k) will be found to contain little of the uncorrelated noise and therefore, performance of the adaptive filter will not be as significantly affected as in the previous case where the uncorrelated noise was applied to the filter's d(k) input.

LMS Filter Parameters. Selection of filter parameters of the LMS adaptive filter have an important influence on filter performance; affecting adaptation speed, weight values and output noise levels. Two of the most important of these parameters are the order of the filter L and the convergence parameter μ. Several methods can be used for selecting these parameters depending upon the information available to the filter designer (2;15;16;17). These methods however are usually used as guidelines for initial

design estimates and optimum filter performance is normally obtained only after operating the filter through several iterations with different additional parameter estimates. Two commonly used formulas used to estimate L and μ are as follows:

For filter order L (15:112;16:214)

$$L = NM - 1 \tag{41}$$

where N is the number of independent training samples and M is the misadjustment. Misadjustment is defined as a measure of how closely the weight vector tracks the optimum weight vector solution. For most applications misadjustment is usually set at 10 percent (15:112).

For the convergence parameter μ, convergence of the weight vector solution is defined by the boundary limits given by (15:103) as

$$0 < \mu < 1/\mathrm{tr}[\underline{R}] \tag{42}$$

where tr[$\underline{R}$] is defined as the sum of the diagonal elements of $\underline{R}$.

Software Implementation of the LMS Adaptive Filter

A software implementation of the LMS adaptive noise cancellation filter was developed using the LMS algorithm defined by Equations (5) and (8). This program was written using Turbo Pascal V4.0 and executes a non-real-time

adaptive filter with a user selectable μ and weight lengths from 2 to 65. A program listing is provided in Appendix E.

LMS Adaptive Filter Performance Test Results

Performance tests were conducted to determine the feasibility of using the LMS adaptive noise cancellation filter to reduce noise artifacts generated by the AAMRL/RCA microwave arterial pulse monitor. Filter performance was evaluated based on the filter's ability to reduce output noise power levels to where the presence/absence of the pulse monitor's pulse signal could be detected. The tests used the software implementation of the LMS adaptive filter contained in Appendix E with the three arterial pulse monitor test signal pairs developed in Chapter 4. Different combinations of filter parameter values for L and μ were evaluated to determine a final filter design which produced the lowest peak output noise power levels. Results of the performance tests were as follows:

Positive Correlation Test. The positive correlation test was conducted using the test signal pair shown in Figure 8. The noise signals in this test signal pair represent noise artifacts generated by opening and closing the mouth five times in succession. Filter order L was calculated using different lengths of training samples and Equation (41) with M set at 10 percent. These different filter order lengths were then inturn used to calculate the upper boundary limits for μ by using Equation (42) and the

noise input from the positive correlation test signal. Results of these calculations (see Table 4) were used as a guideline for selecting filter parameter combinations of L and μ for evaluation. A list of these parameter combinations evaluated during the test are cross referenced in Table 5.

Table 4. Filter Order L and μ max Versus Number of Training Samples N for the Positive Correlation Test Signal Pair

Training Sample Length (N)	Filter Order (L)	tr[R]	μ max
20	1	0.5823	1.7173
40	3	1.1184	0.8941
60	5	1.3662	0.7320
80	7	1.8798	0.5320
100	9	2.2944	0.4358
200	19	2.8434	0.3517
300	29	3.1692	0.3155

Table 5. Evaluation Cross Reference for L and μ for the Positive Correlation Test

μ	Filter Order (L)					
	3	5	7	9	19	29
0.1		X		X	X	X
0.2		X	X	X	X	X
0.3		X	X	X	X	X
0.4		X	X	X		
0.5		X	X			
0.6	X	X				
0.7	X	X				
0.8	X					
0.9	X					

Overall, performance of the adaptive filter was extremely poor for the L and μ combinations evaluated. Results showed little improvement between filter's input and output noise levels with results best described as trading one set of noise for another. Best filter performance was obtained by using the larger μ values for each filter order category tested. Results of the evaluation showed a fifth order filter with μ set at 0.7 produced the lowest peak output noise power levels. This result is shown in Figure 13 as a normalized comparison of the d(k) input power level versus the filter output level. Examination of these plots shows a slight decrease between the peak input and output power levels with a tapering off of the peak power levels as the adaptive filter begins to adapt on the three subsequent transient noise pulses. Although this performance appears encouraging, by the time of the fifth transient pulse the input noise correlation (see Figure 8) has changed enough to cause the filter to readapt and thereby increase the output noise power level to almost the same level as in the input. Additional insight on the performance of this filter combination for L and μ can be obtained in Figure 14 where the actual signal-plus-noise output for the filter is provided for comparison along with the filter's W0 weight value plot. In this figure, the W0 weight value plot shows initial adaptation of W0 to an approximate steady state value of 0.3 for the first 3 transient pulses. Unlike the

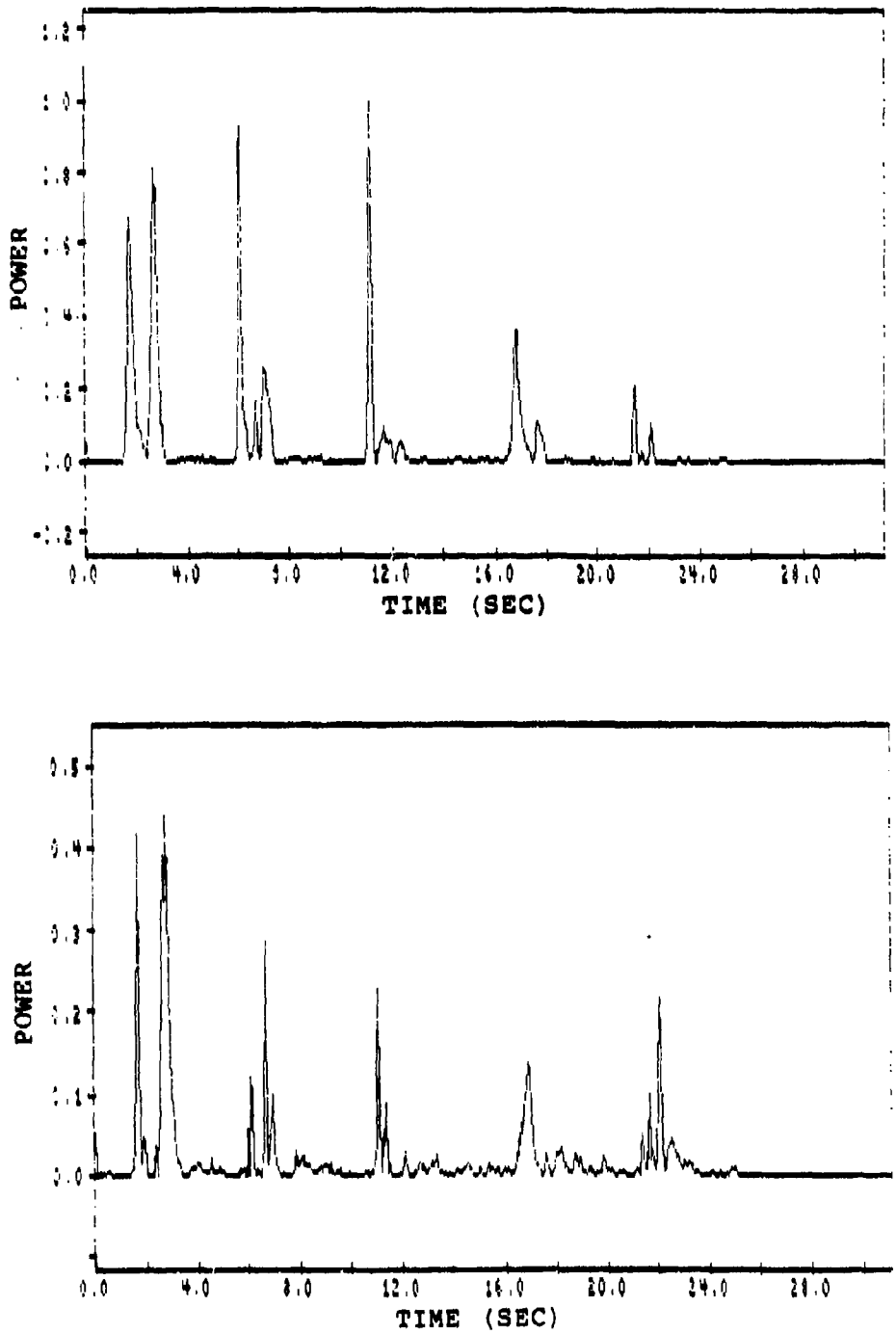

Figure 13. Positive Correlation Test, Normalized Filter Power Levels, Input (top), Output (bottom)

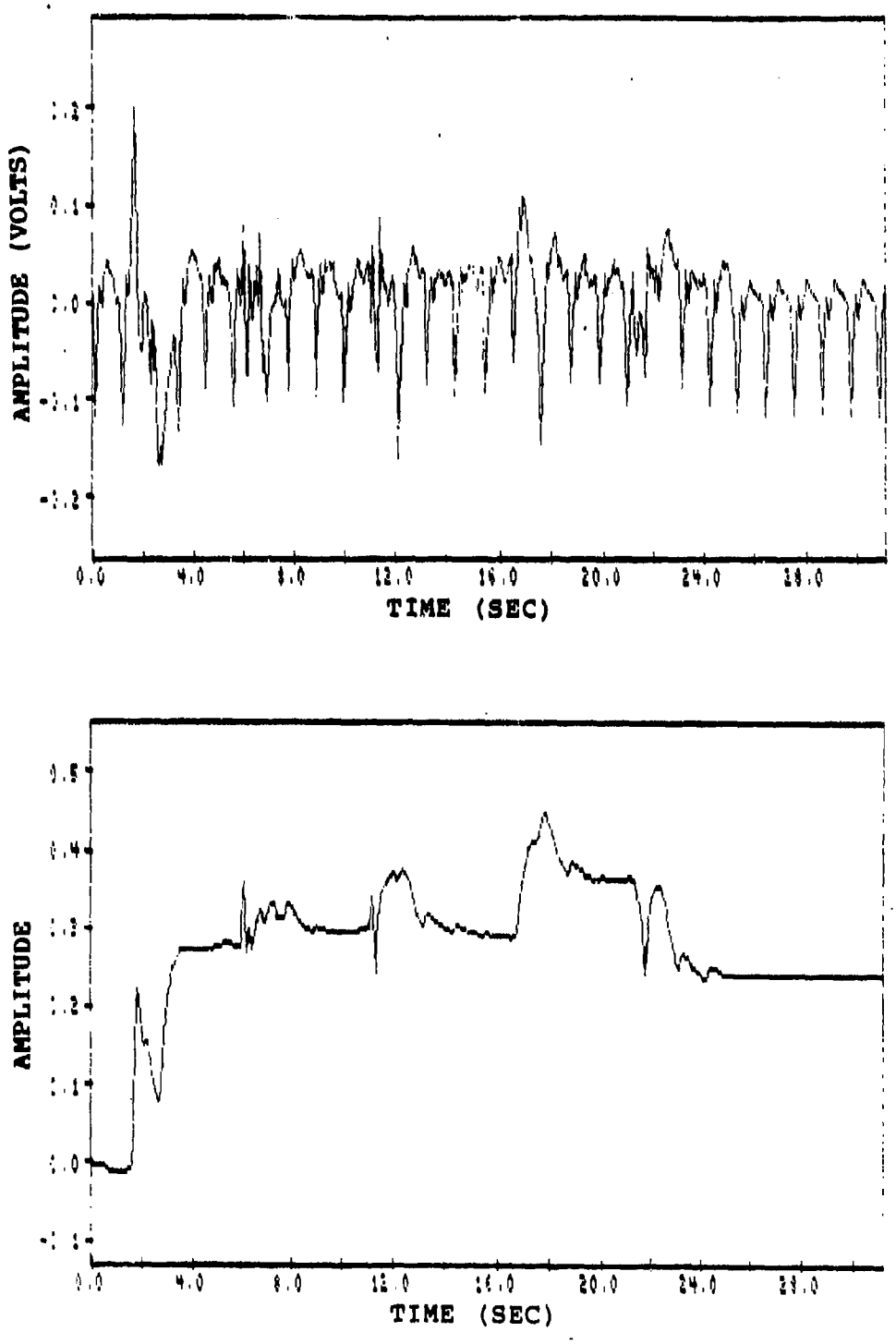

Figure 14. Positive Correlation Test, Filter Signal-Plus-Noise Output (top), Filter Weight W0 (bottom)

previous assessment however, the W0 weight is shown to begin to readapt on the fourth pulse to a new higher steady state value. This readaptation is then suddenly followed by another adaptation where W0 decreases and then increases during the occurrence of the fifth pulse. This behavior of weight W0 is indicative of the filter weight vector attempting to track a changing optimum weight vector solution. This changing optimum weight vector solution is caused by nonstationary input signals. The effects of nonstationary signals on the adaptive filter was previously discussed in the filter theory section of this thesis.

Negative Correlation Test. The negative correlation test was conducted using the test signal pair shown in Figure 9. The noise signals in this test signal pair represent noise artifacts generated by biting/gritting the teeth together two times in succession. Filter order L was calculated using different lengths of training samples and Equation (41) with M set at 10 percent. These different filter order lengths were then inturn used to calculate the uppe boundary limits for μ by using Equation (42) and the noise input from the negative correlation test signal. Results of these calculations (see Table 6) were used as a guideline for selecting filter parameter combinations of L and μ for evaluation. A list of these parameter combinations evaluated during the test are cross referenced in Table 7.

Table 6. Filter Order L and μ max Versus Number of Training Samples N for the Negative Correlation Test Signal Pair

Training Sample Length (N)	Filter Order (L)	tr[R]	μ max
20	1	0.7041	1.4203
40	3	1.3460	0.7429
60	5	1.8598	0.5377
80	7	2.2292	0.4486
100	9	2.5251	0.3960
200	19	3.7077	0.2697
300	29	4.6057	0.2171

Table 7. Evaluation Cross Reference for L and μ for the Negative Correlation Test

μ	Filter Order (L)						
	1	3	5	7	9	19	29
0.1		X		X	X	X	X
0.2		X	X	X	X	X	X
0.3		X	X	X	X		
0.4		X	X	X	X		
0.5		X	X				
0.6	X	X					
0.7	X	X					
0.8	X						
0.9	X						
1.0	X						
1.2	X						
1.3	X						

Performance of the adaptive filter with the negative correlation signal pair was similar to the results obtained for the positive correlation test. Results were extremely poor for all the L and μ combinations evaluated and like the observation made previously for the positive correlation test, results can be best described as trading one set of

noise for another. Best filter performance was obtained by using the larger μ values for each filter order category tested which was in agreement with the positive correlation test results. Unlike the previous results however, the evaluation showed a third order filter with μ set at 0.7 produced the lowest peak output noise power levels. This result is shown in Figure 15 as a normalized comparison of the d(k) input power level versus the filter output level. Examination of these plots shows an order of magnitude decrease between the peak input and output power levels for the first transient noise response. The second transient noise response also showed a decrease in the output power levels, although not as significant as for the first pulse. This difference can probably be attributed to a time lag change (correlation change) between the x(k) and d(k) inputs of the filter for the two different transient pulses evaluated (see Figure 9). This change in correlation affects the adaptation of the filter and hence, the filter's level of output noise for a given input. Additional insight on the performance of this filter combination for L and μ can be obtained in Figure 16 where the actual signal-plus-noise output for the filter is provided for comparison along with the filter's W0 weight value plot. In this figure, the W0 weight value plot shows during the first transient pulse, an initial rapid adaptation of W0 to an approximate negative peak 1.25 followed an almost equally rapid decline to a

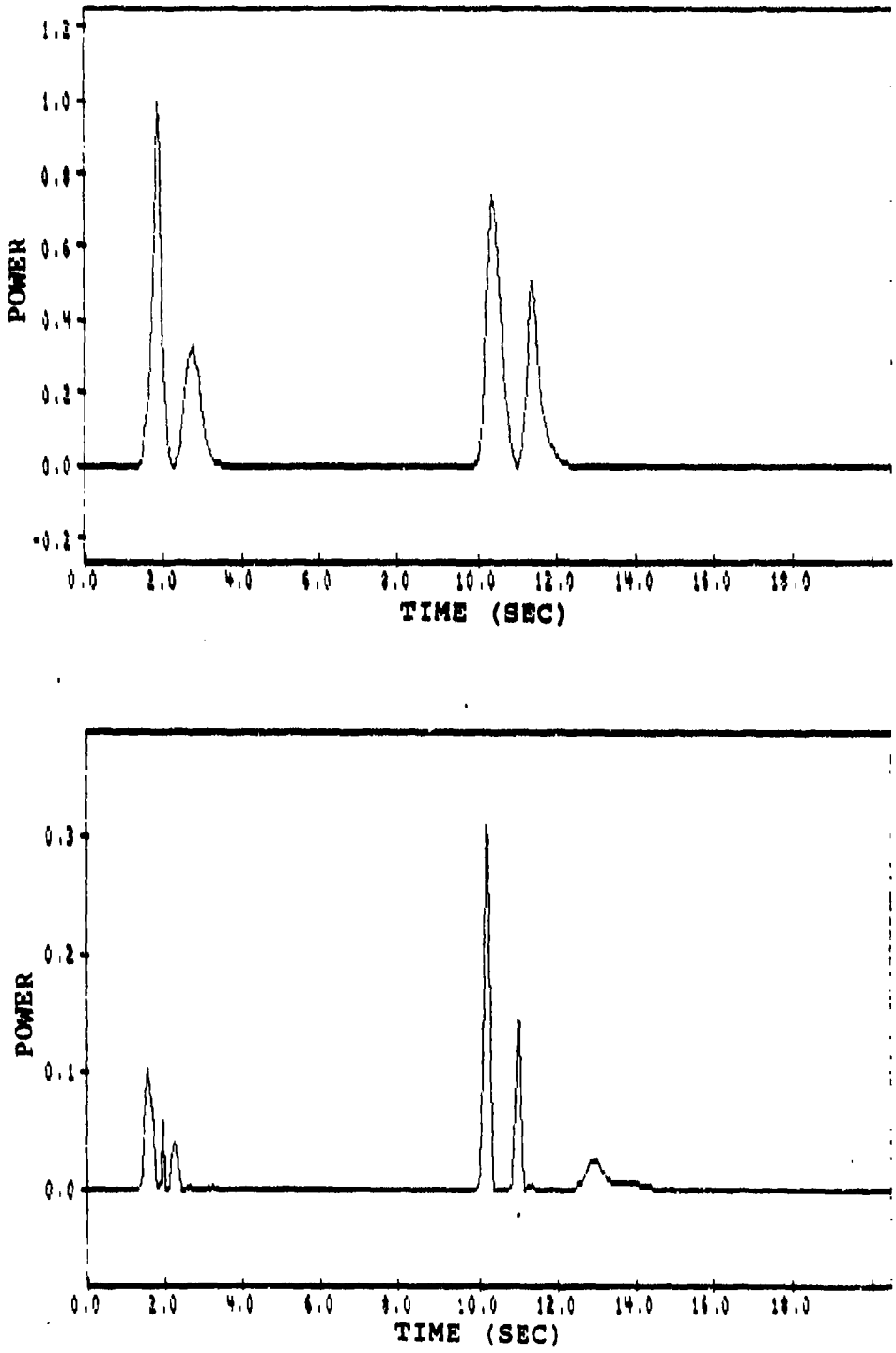

Figure 15. Negative Correlation Test, Normalized Filter Power Levels, Input (top), Output (bottom)

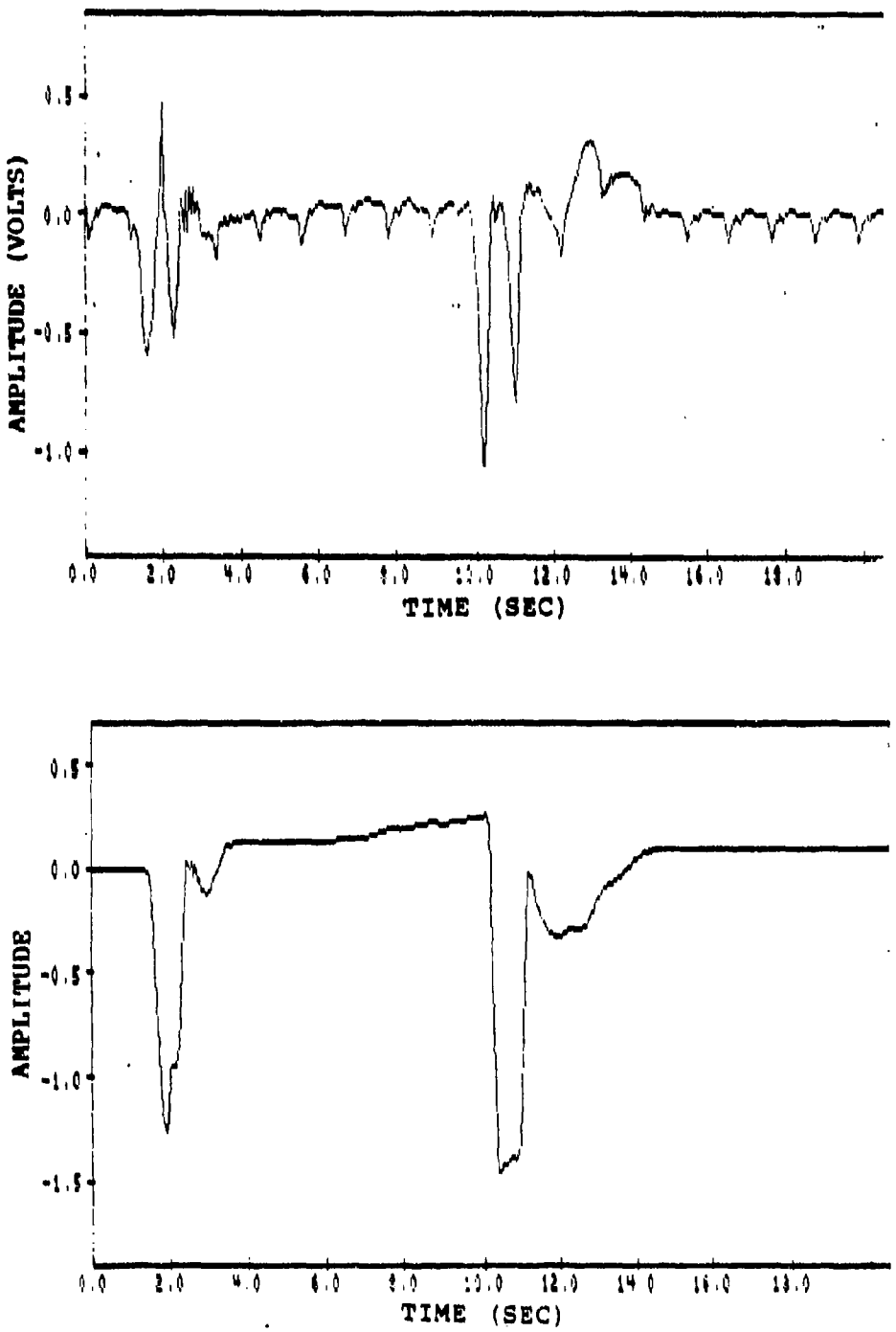

Figure 16. Negative Correlation Test, Filter Signal-Plus-Noise Output (top), Filter Weight W0 (bottom)

steady state value of 0.1 . A similar performance is also observed for the second transient pulse. This performance with the widely varying weight W0 over the period of the transient pulse indicates a time varying optimum weight vector solution which is characteristic of a nonstationary signal. The effects of nonstationary signals on the adaptive filter was previously discussed in the filter theory section of this thesis.

Intermittent Correlation Test. The intermittent correlation test was conducted using the test signal pair shown in Figure 10. The noise signals in this test signal pair represent noise artifacts generated by counting to ten. Filter order L was calculated using different lengths of training samples and Equation (41) with M set at 10 percent. These different filter order lengths were then inturn used to calculate the upper boundary limits for μ by using Equation (42) and the noise input from the negative correlation test signal. Results of these calculations (see Table 8) were used as a guideline for selecting filter parameter combinations of L and μ for evaluation. A list of these parameter combinations evaluated during the test are cross referenced in Table 9.

Performance of the adaptive filter with the intermittent correlation signal pair was similar to the results obtained for the positive and negative correlation tests. Results were extremely poor for all the L and μ

Table 8. Filter Order L and μ max Versus Number of Training Samples N for the Intermittent Correlation Test Signal Pair

Training Sample Length (N)	Filter Order (L)	tr[R]	μ max
20	1	0.3589	2.7863
40	3	0.5967	1.6759
60	5	0.6800	1.4706
80	7	0.6989	1.4308
100	9	0.7065	1.4154
200	19	0.7744	1.2913
300	29	0.8441	1.1847

Table 9. Evaluation Cross Reference for L and μ for the Intermittent Correlation Test

μ	Filter Order (L)						
	1	3	5	7	9	19	29
1.1		X		X	X	X	X
1.2		X	X	X	X	X	X
1.3		X	X	X	X	X	
1.4		X	X	X	X		
1.5	X	X	X				
1.6	X	X					
1.7	X						
2.0	X						
2.3	X						
2.7	X						
1.2	X						
1.3	X						

combinations evaluated and like the previous test observations, results were once again, best described astrading one set of noise for another. Best filter performance was again obtained by using the larger μ values for each filter order category tested. Unlike the previous results however, this evaluation showed a third order filter with μ set at 1.6 produced the lowest peak output noise

power levels. This result is shown in Figure 17 as a normalized comparison of the d(k) input power level versus the filter output level. Examination of these plots shows an inconclusive set of results, with some reduction in power levels between the filter's x(k) input and output. Additional insight on the performance of this filter combination for L and μ can be obtained in Figure 18 where the actual signal-plus-noise output for the filter is provided for comparison along with the filter's W0 weight value plot. In this figure, the W0 weight value plot shows a random time varying weight value. This behavior of weight W0, like the previous observations is indicative of the filter weight vector attempting to track a changing optimum weight vector solution which is characteristic of a nonstationary signal. The effects of nonstationary signals on the adaptive filter was previously discussed in the filter theory section of this thesis.

Adaptive Filter Performance Evaluation. Performance of the LMS adaptive filter on the three sets of test signal pairs was extremely poor. Results showed no significant reduction between the noise at the input to the filter and its output. This result was attributed to the almost constantly changing filter weight vector caused by the nonstationary input test signals. These input signals were identified as nonstationary during the test because they occurred at random times and were transient. In addition,

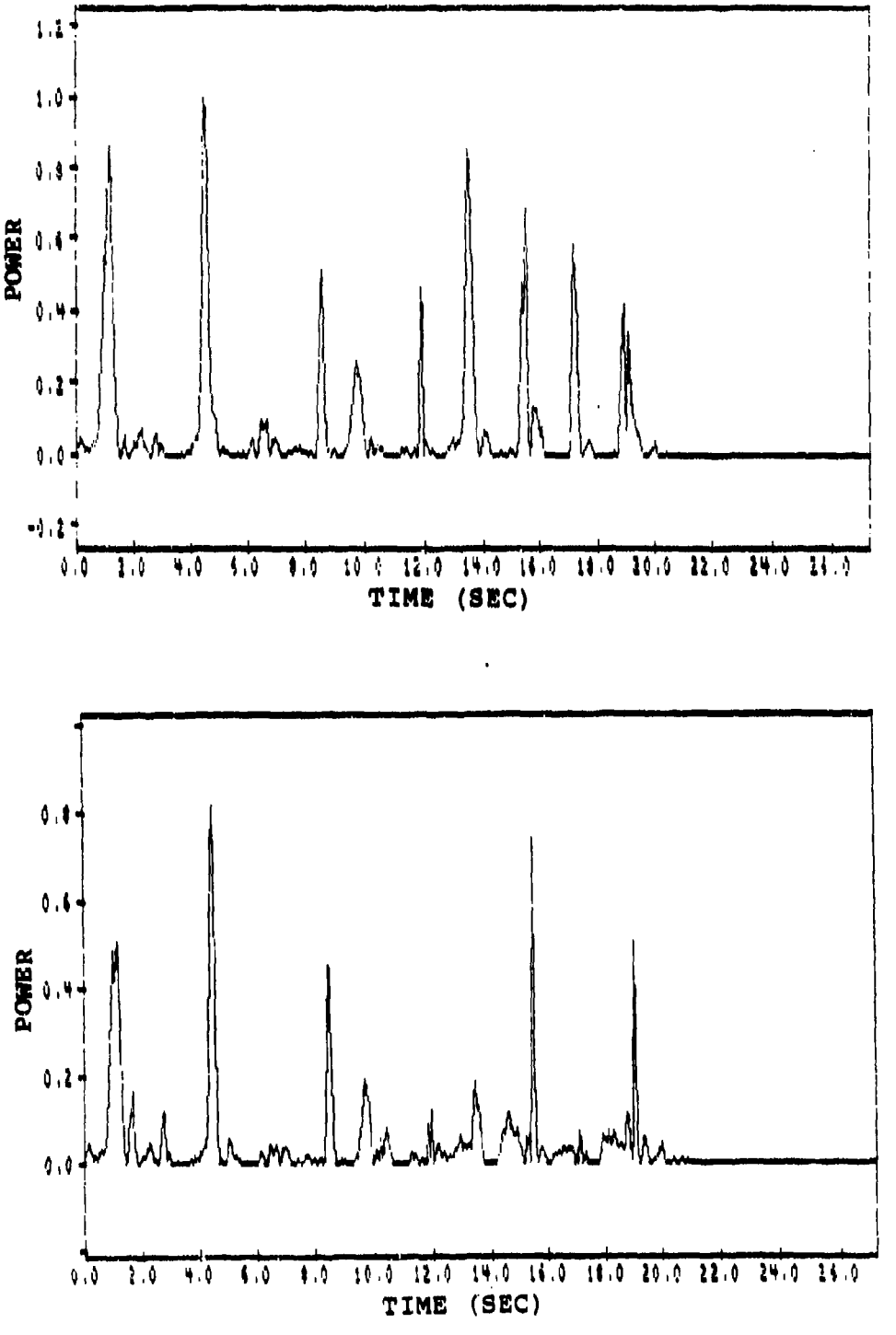

Figure 17. Intermittent Correlation Test, Normalized Filter Power Levels, Input (top), Output (bottom)

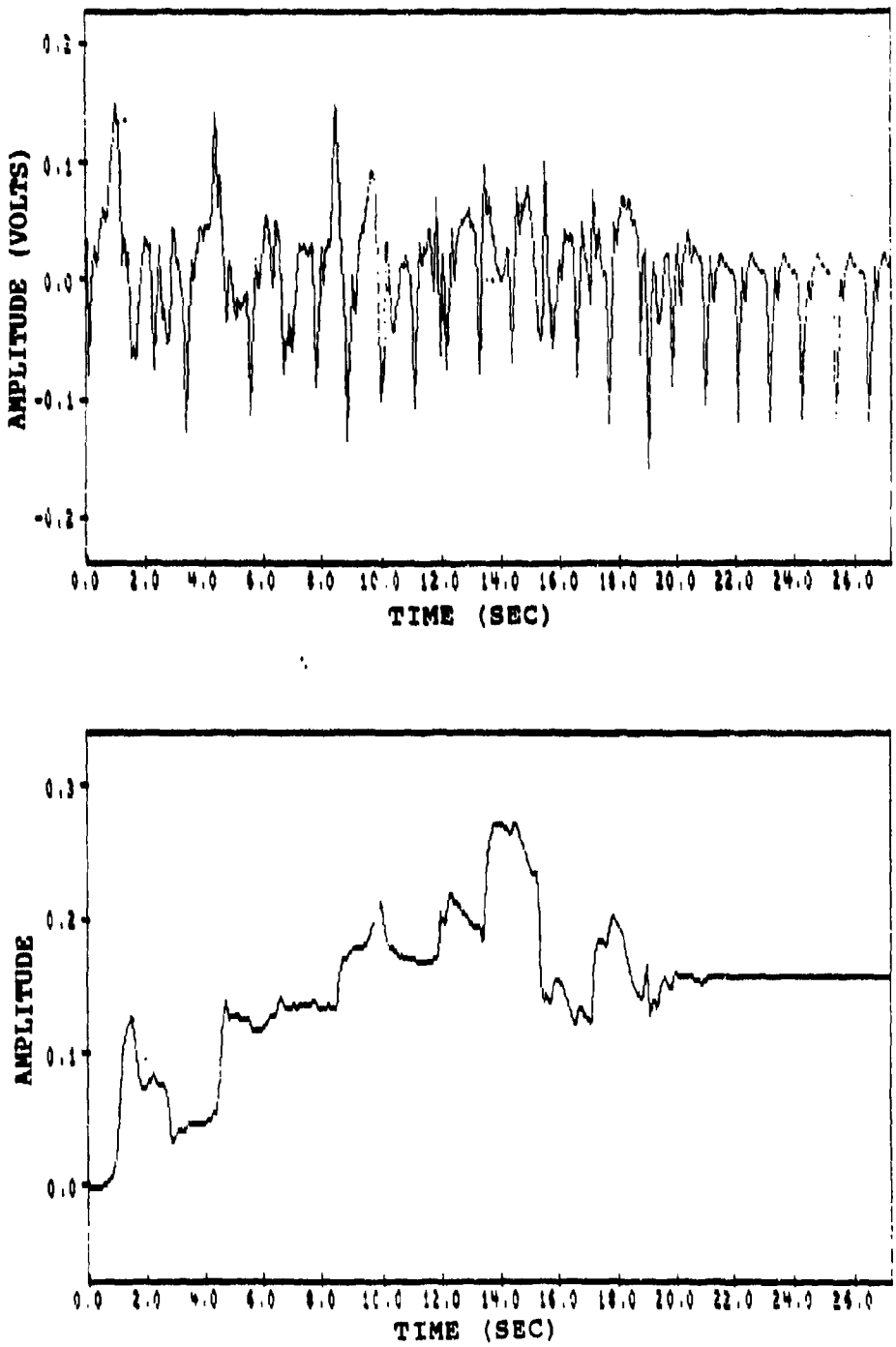

Figure 18. Intermittent Correlation Test, Filter Output (top), Filter Weight W0 (bottom)

over the duration of most of these transient pulses, the correlation between the inputs was varying and never seemed to converge to any fixed value. Both of these characteristics cause severe problems for the LMS filter and were probably the most significant reasons for the poor filter performance.

In order for the LMS adaptive noise cancellation filter to work properly, two major conditions must be met. The first condition requires a certain degree of signal stationarity over several periods of transient pulse signals so the filter can converge to an optimum weight vector solution which minimizes output noise. The second condition requires a fairly constant degree of correlation between the noise inputs to the filter. Since neither of these conditions are satisfied by the noise outputs of the current AAMRL/RCA arterial pulse monitor, the use of LMS adaptive noise cancellation filter is not feasible for noise reduction and should therefore not be used.

VI. System Model

Subject-Monitor-Filter System Model

A system model was developed for the subject-monitor-filter system interface using results from the pulse monitor and adaptive filter evaluation. This system model is shown in Figure 19 and consists of three parts: the subject, the monitor and the filter.

The subject part of the model consists of two separate inputs, signal s and noise n. The signal input originates from the pulsatile motion of blood flow near the surface of the test subject's skin. This signal is corrupted by additive noise caused by movement of the test subject's bone and/or body tissue. The noise input is transient and originates from a common source inside the test subject's head. This noise source represents initiation of an action which will cause movement of the subject's bone and/or body tissue and is applied directly to two time variable transfer functions with different characteristics. These transfer functions are modeled differently because they are dependent on the pulse monitor's transducer locations and the types of tissue and bone movement observed within each of the transducer's movement detection ranges. The effects of these two transfer functions on the noise input is variable and can provide nonlinear outputs with differences in amplitude, frequency and phase.

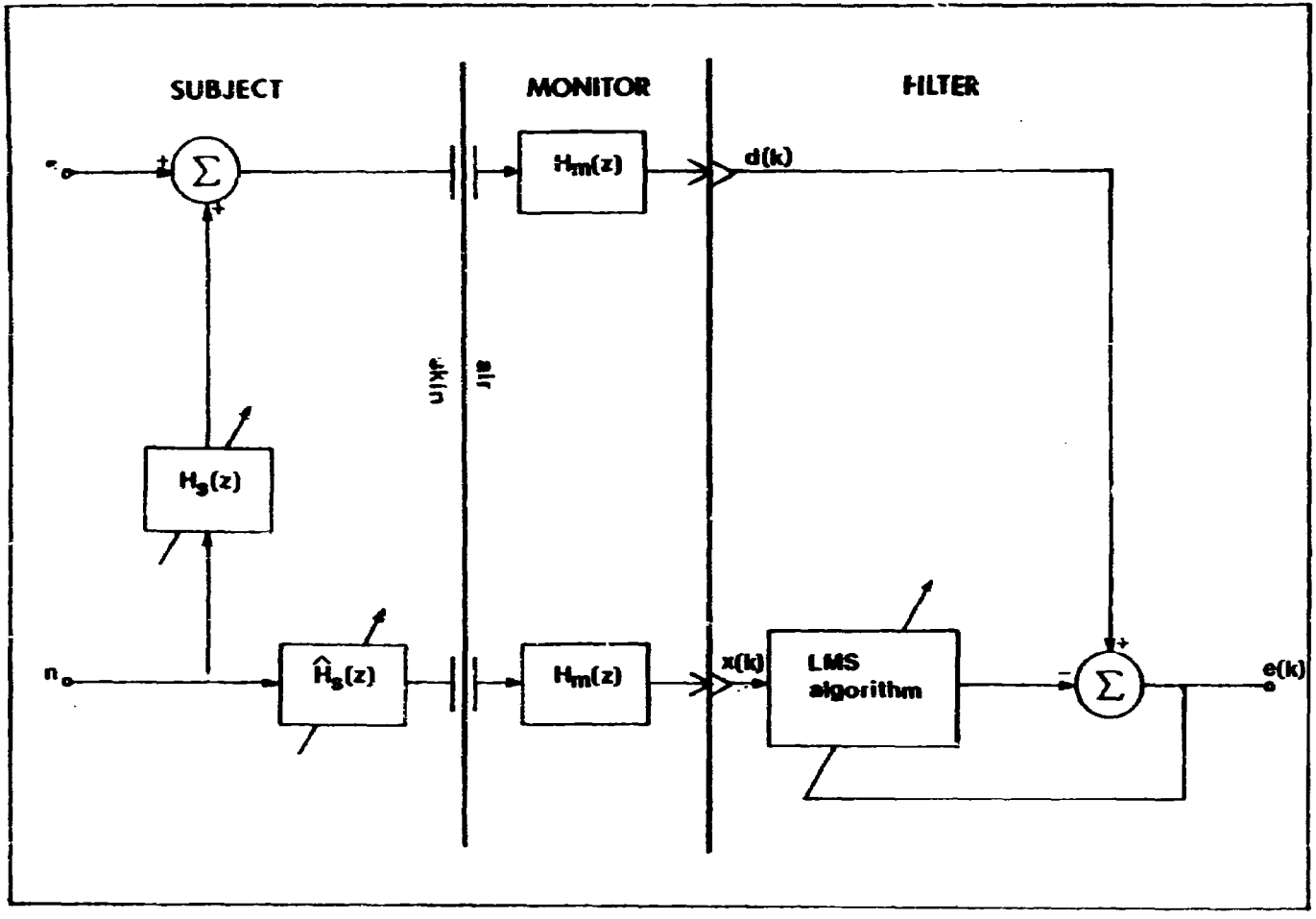

Figure 19. Subject-Monitor-Filter System Model

The monitor part of the model consists of two separate inputs provided at the surface of the test subject's skin. One input consists of signal-plus-noise and the other input noise only. These two inputs are acquired by the pulse monitor through a skin-air-pulse monitor transducer interface in which no additional noise is introduced (see Chapter 1, thesis assumption 4). These inputs are applied to two identical linear transfer functions which perform amplification and low pass filtering, and provide outputs directly to the LMS filter.

The filter part of the model consists of a LMS adaptive noise cancelation filter previously described in this thesis. Its inputs are provided by two pulse monitors and consist of a signal-plus-noise channel d(k) and a noise only channel x(k). The LMS filter output e(k) is obtained by subtracting the adaptively filtered x(k) noise input from the d(k) signal-plus-noise output.

VII. Conclusions and Recommendations

Conclusions

Performance characteristics of the pulse monitor did not vary significantly during the entire evaluation and modification process. A significant amount of development work remains to be accomplished on the pulse monitor to reduce noise artifacts if the pulse monitor is ever expected to find applications outside a controlled laboratory environment. Performance of the pulse monitor was moderately enhanced by the modifications with a slight reduction in noise levels and a reduction in the number of instances of amplifier saturations. Performance characteristics observed using the pulse monitor evaluation setup on test subjects were repeatable with the most significant test finding being the existence of the dual positive/negative going pulse signal. Noise artifacts generated by facial movement of test subjects were found to be transient, nonperiodic and generally uncorrelated from artifact-to-artifact and sensor-to-sensor. These results translated into a highly nonstationary set of signals for the adaptive filter to work with.

Performance of the LMS adaptive noise cancellation filter during the evaluation was extremely poor and was marked by filter weights continually adapting and readapting during each transient noise pulse. This poor performance

was caused by the highly nonstationary noise inputs to the filter which produced an almost constantly varying optimum weight vector solution and hence a noisy filter output. Although the evaluation showed the filter reduced peak input noise power levels, the filter's output still contained a significant amount of noise and the overall effect of the filtering process was characterized as exchanging one set of noise for another. As a result of this, the use of the LMS adaptive noise cancellation filter was determined to be not feasible for noise reduction use with the AAMRL/RCA pulse monitor.

Recommendations

No further follow on LMS adaptive filter evaluation work is recommended due to the highly nonstationary noise characteristics observed with the present configuration of the AAMRL/RCA pulse monitor.

Additional work should be concentrated on further design enhancements to the pulse monitor's transducer assembly. These enhancements should include work in the transducer-to-subject mounting techniques, reduction in the transducer-to-subject air gap, miniaturization of the transducer assembly and improvements in the transducer's cable shielding/grounding.

Appendix A

Experimental Data Collection Sheets

The following two pages contain the experimental data collection sheets used to log in results of each experiment. Two types of data collection sheets were used, noise correlation data sheets and sensor test data sheets.

Noise correlation data sheets were used to log in results two channel noise data experiments. The purpose of the noise correlation experiments were to record two channels of noise only data (no pulse signal present) for use in correlation studies. These studies were to be used to determine the optimum location to place the pulse monitor sensors to record test signals for adaptive filter evaluation. Due to the limited success in finding correlated two channel noise only data sources this data sheet saw minimal use.

Sensor data sheets were used to log in the results of all the remaining experiments not related to the noise correlation experiments. These remaining experiments primarily consisted of collecting either two channels of signal-plus-noise data or simultaneously collecting a single channel of noise data and a single channel of signal-plus-noise data. The majority of the data used in this thesis for evaluation, analysis and test was collected using this data sheet.

Noise Correlation Data Sheet

Date: _____
Sheet: _____
Disk(s): _____
Data Rate: _____
Analog Filter (Fco): _____

Subject: _____
Sensor Position: 1 2 3 4

Data Channel ID:
Channel 1: _____
Channel 2: _____

Sensor Orientation:
_____
_____

DATA	DURATION (sec)	EVENT #
1. Yawn	20	____
2. Swallow	20	____
3. Open/close mouth	20	____
4. Bite/grit teeth	20	____
5. Count to ten	20	____
6. Eye blinks		
a. Soft	20	____
b. Hard	20	____
7. Eye movement		
a. Left - Right - Left	20	____
b. Level - Up - Level	20	____
c. Level - Down - Level	20	____

Notes:

Sensor Test Data Sheet

Date: _____
Sheet: _____
Disk(s): _____
Data Rate: _____
Analog Filter (Fco): _____

Subject: _____
Sensor Position: 1 2 3 4

Data Channel ID:
Channel 1: _____
Channel 2: _____

Sensor Orientation:
_____
_____

DATA	DURATION (sec)	EVENT #
1. Subject resting	60/____	____
2. Yawn	20	____
3. Swallow	20	____
4. Open/close mouth	20	____
5. Bite/grit teeth	20	____
6. Count to ten	20	____
7. Read phrase aloud	60/____	____
8. Eye blinks		
a. Soft	20	____
b. Hard	20	____
9. Eye movement		
a. Left - Right - Left	20	____
b. Level - Up - Level	20	____
c. Level - Down - Level	20	____
10. Random noise (repeat items 1 - 9 in a random fasion)	120/____	____

Notes:

Appendix B

Temporal Signal Waveforms

The following four pages contain typical examples of pulse signals recorded from temporal regions 1 through 4 along with their respective 1024 point power spectral densities.

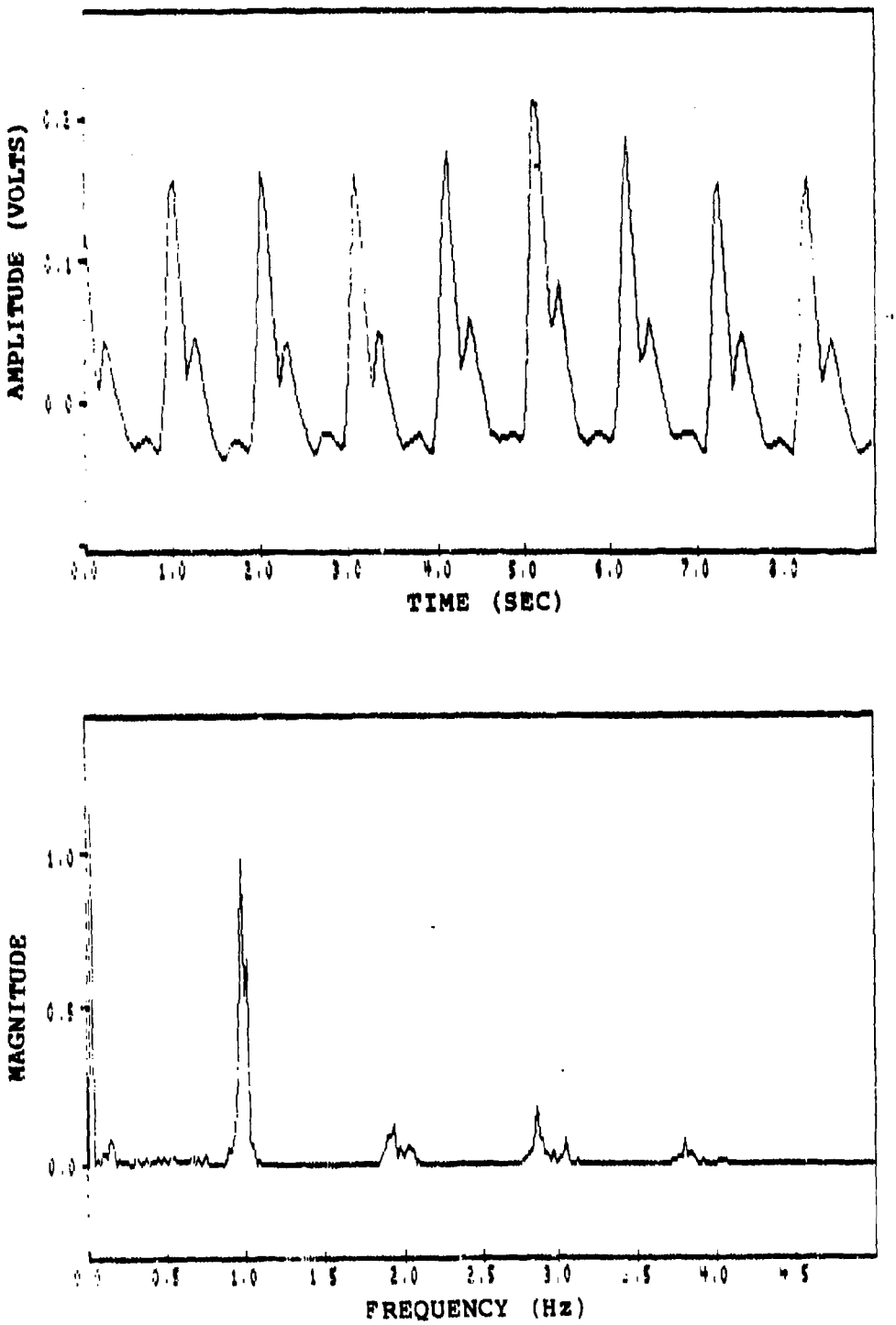

Figure 20. Region 1 Pulse Signal (top) and its Power Spectral Density (bottom)

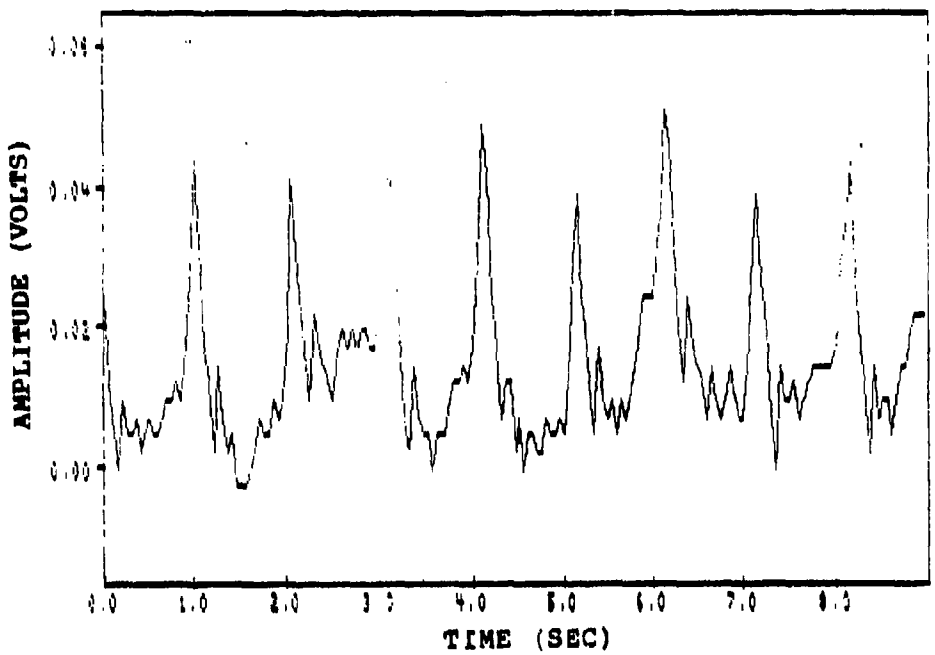

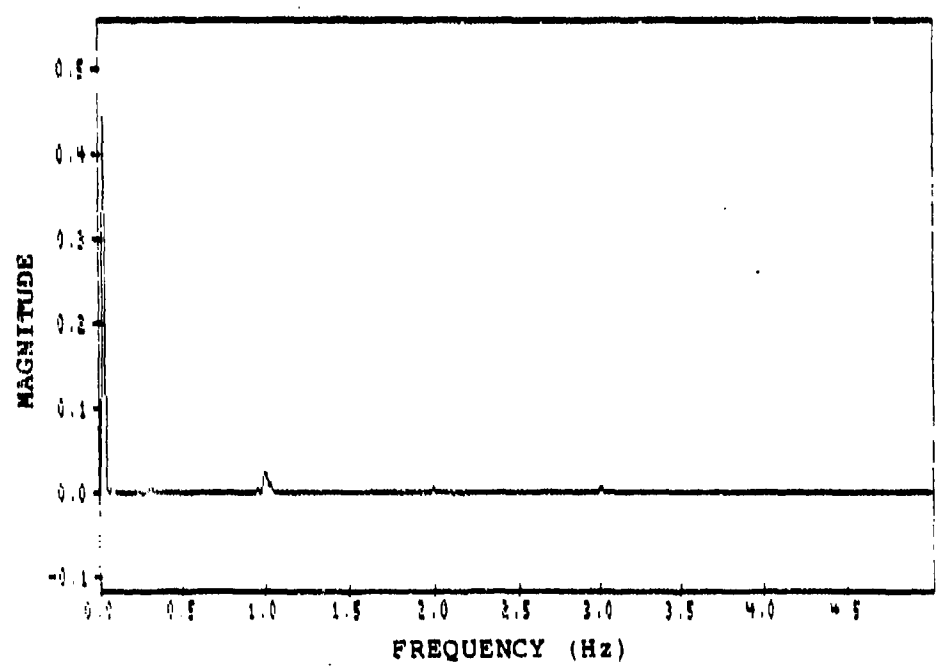

Figure 21. Region 2 Pulse Signal (top) and its Power Spectral Density (bottom)

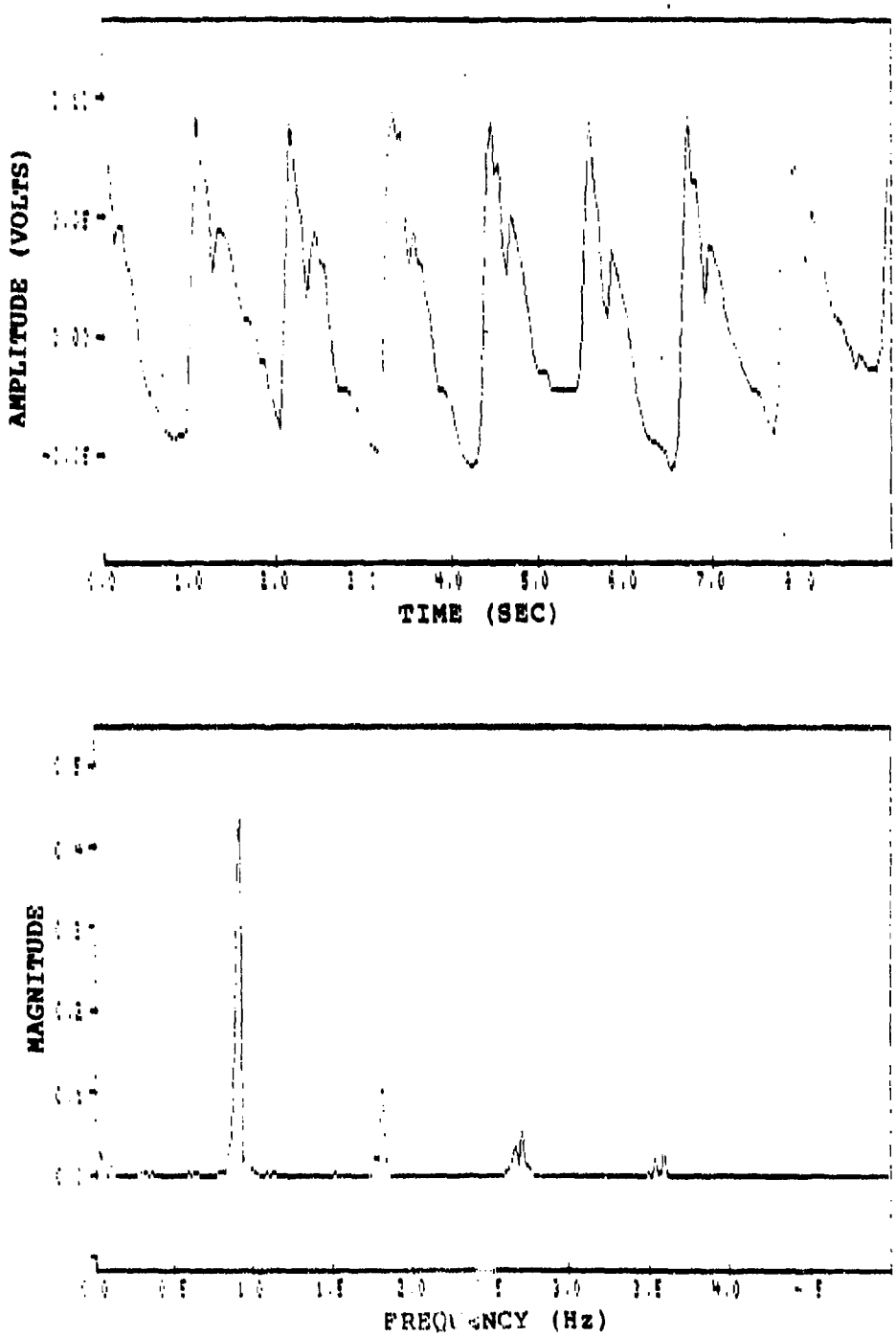

Figure 22. Region 3 Pulse Signal (top) and its Power Spectral Density (bottom)

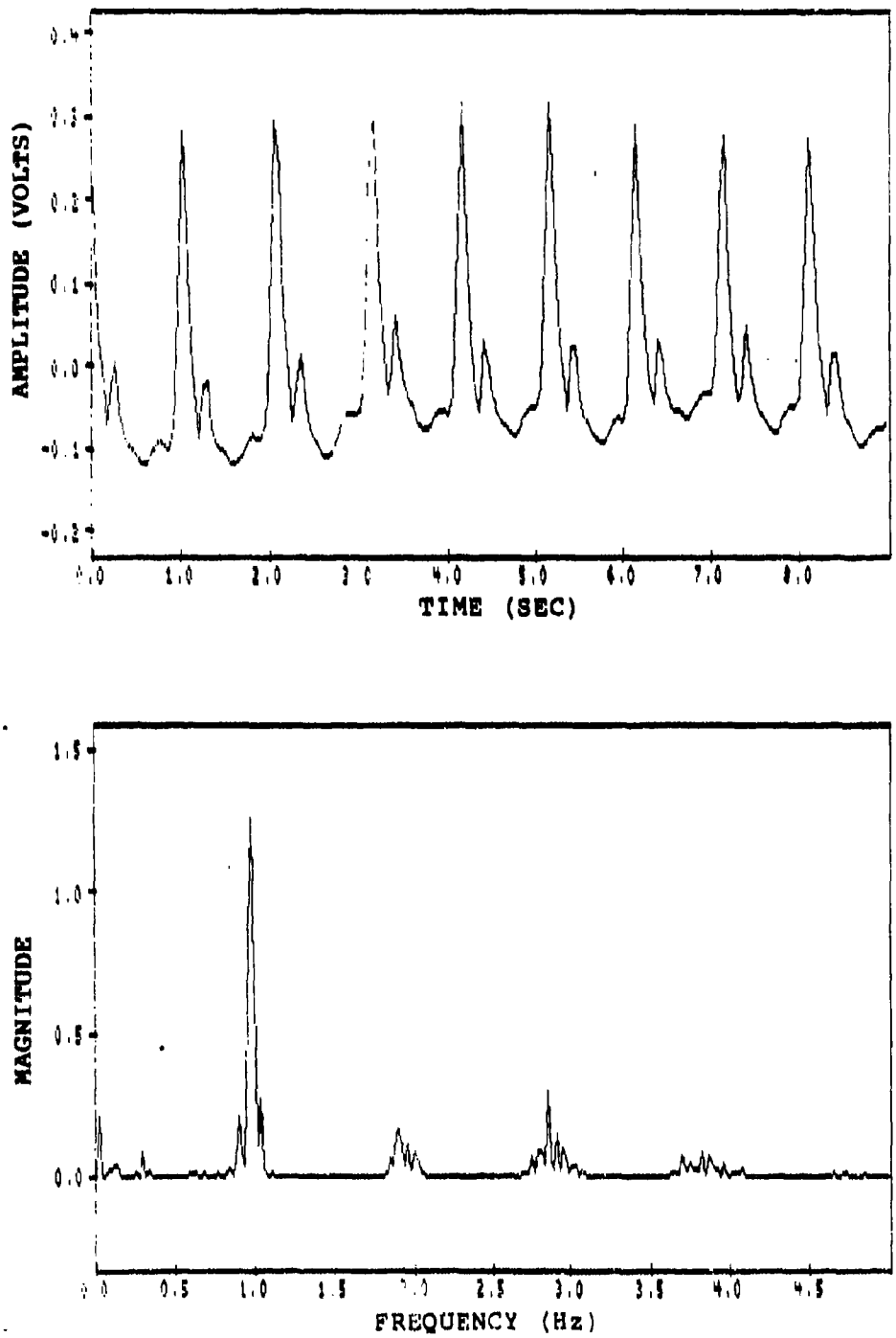

Figure 23. Region 4 Pulse Signal (top) and its Power Spectral Density (bottom)

Appendix C

Example Noise Correlation Data Run

The following seven pages contain an example of a noise correlation data run. The data collection configuration used was the pulse monitor evaluation setup, optimum configuration, with gain set at 184.5. Each figure shows the noise output for a pair of pulse monitor sensors mounted on a test subject's left and right temporal region 3. Comparison of the top and bottom plots in each figure illustrates some of the differences recorded between the left and right channels. Significant features of each pair of plots are listed as follows:

1. Figure 24. Intermittent correlation between plots.
2. Figure 25. Negative correlation and variation in amplitude between plots.
3. Figure 26. Positive correlation, variation in amplitude and change of pulse to pulse correlation between plots.
4. Figure 27. Negative correlation and variation in amplitude between plots.
5. Figure 28. Intermittent correlation between plots.
6. Figure 29. Lack of correlation between plots.
7. Figure 30. No correlation between plots.

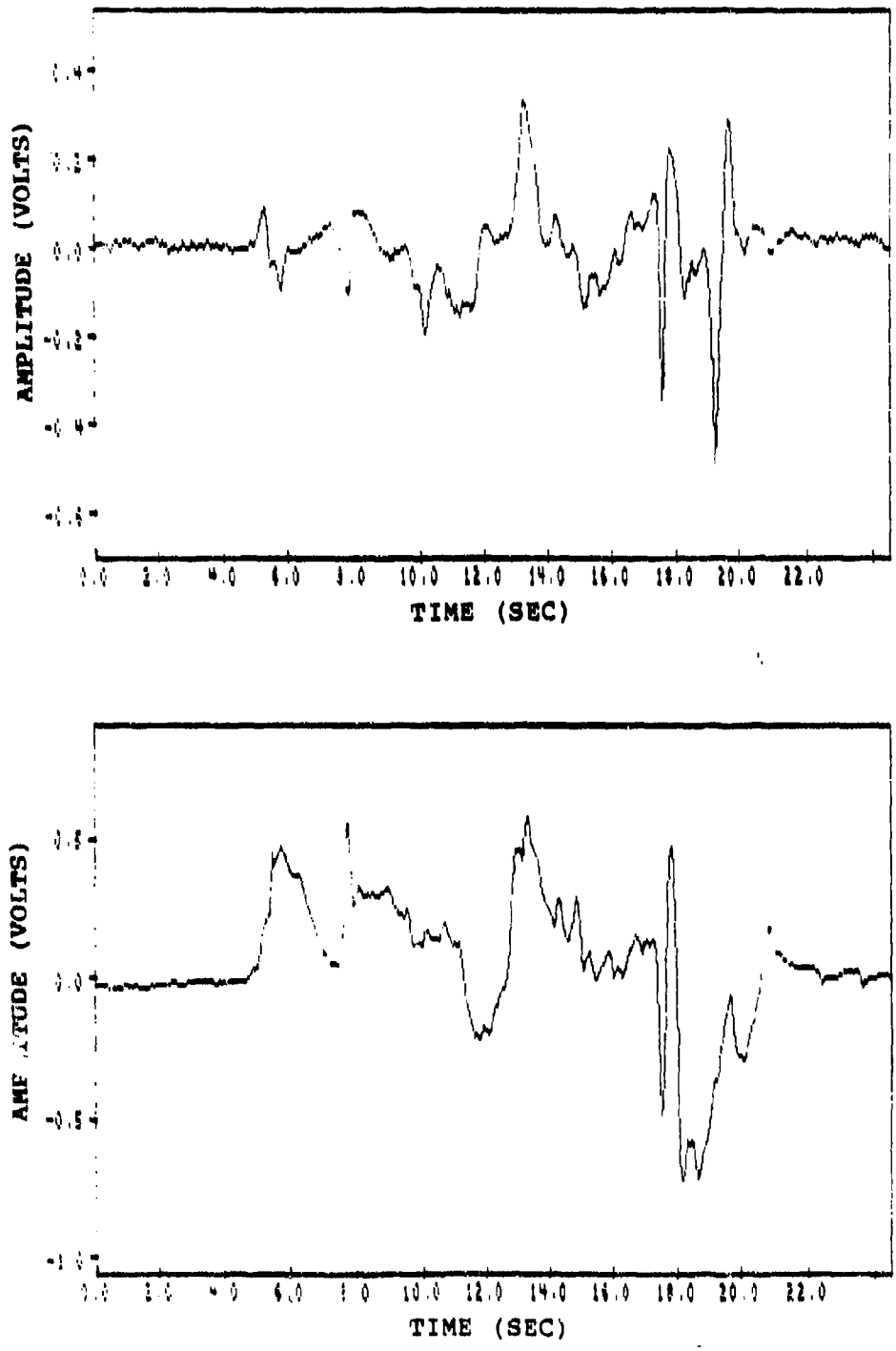

Figure 24. Two Yawns; Left Channel (top), Right Channel (bottom)

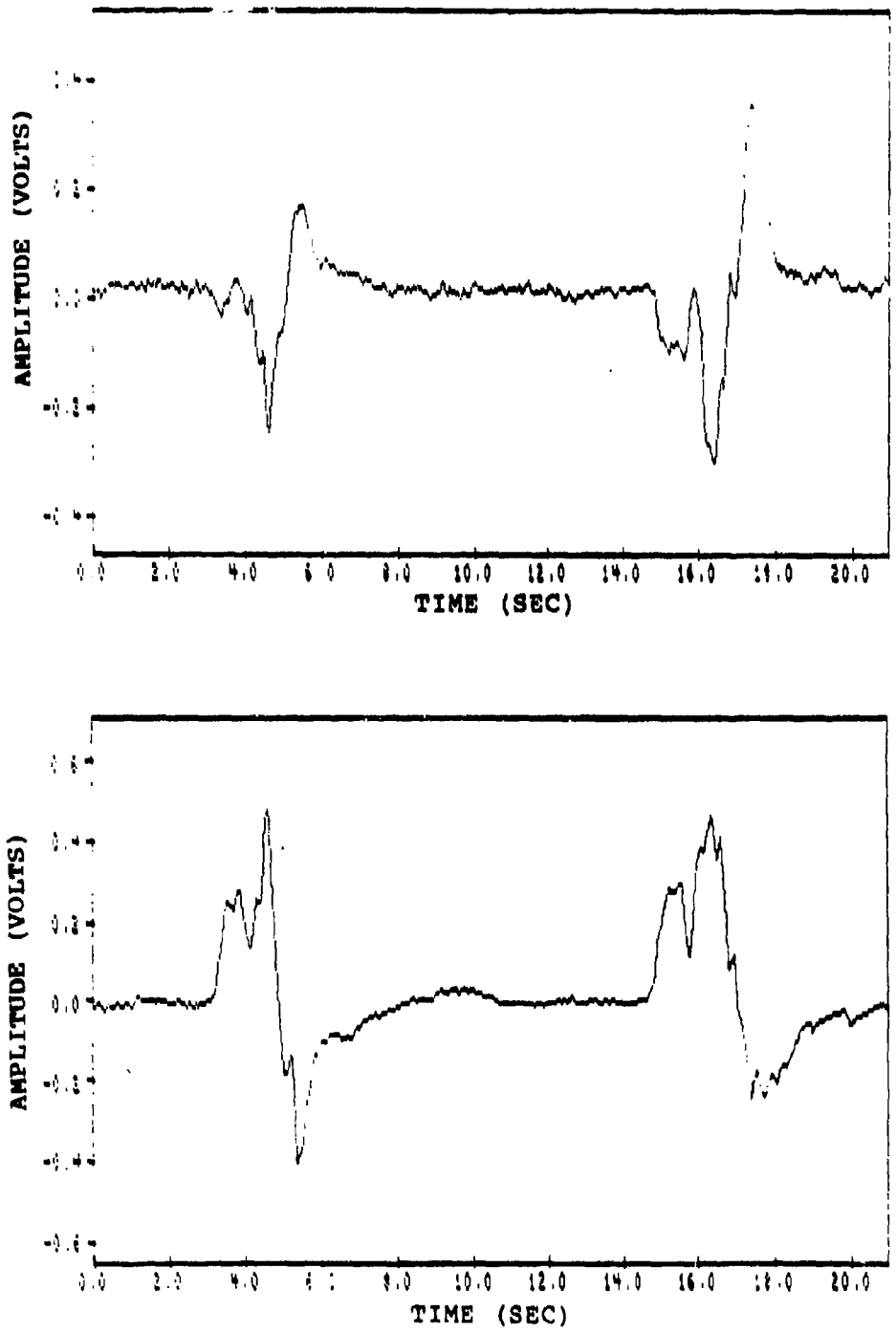

Figure 25. Two Swallows; Left Channel (top), Right Channel (bottom)

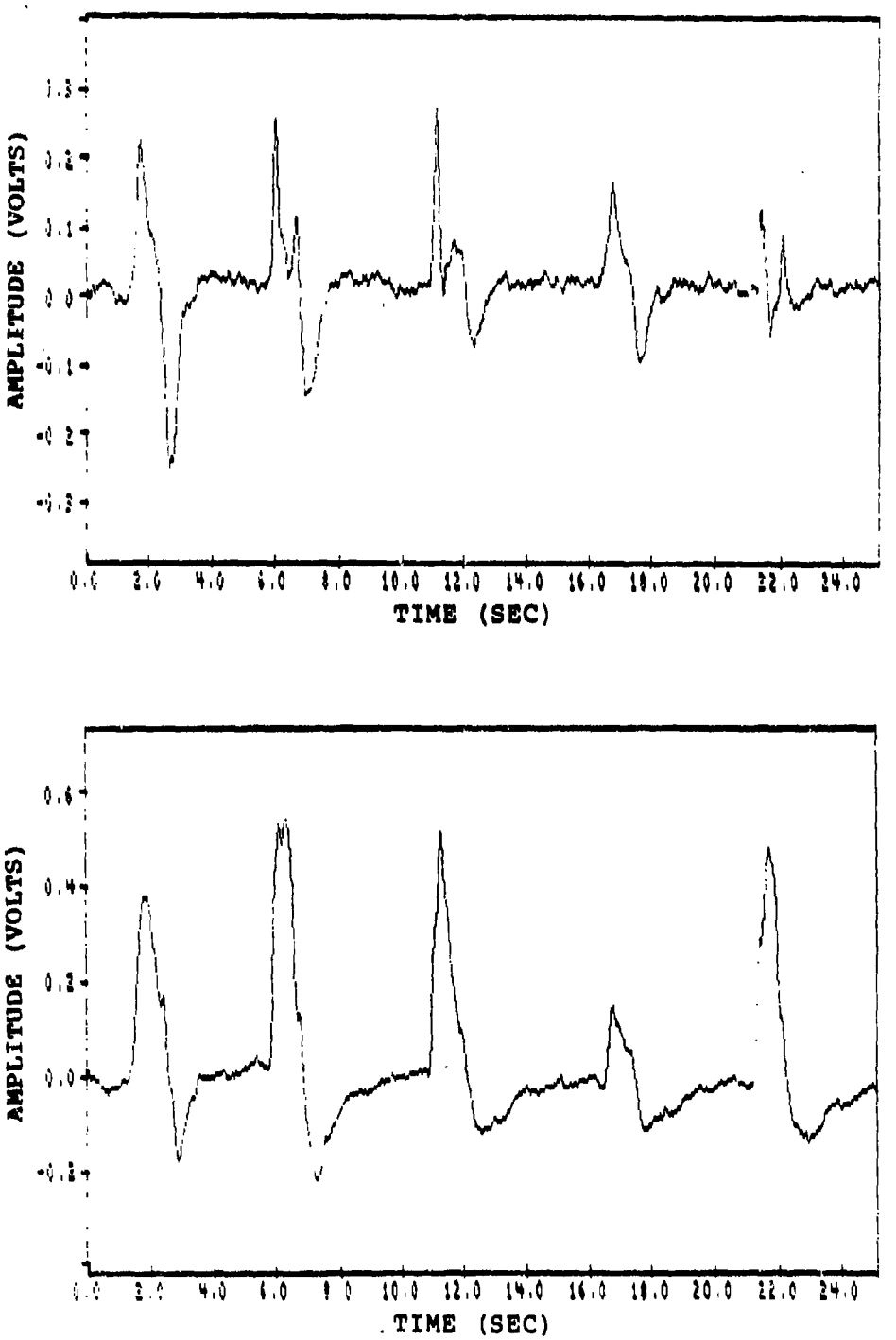

Figure 26. Open/Close Mouth Five Times; Left Channel (top), Right Channel (bottom)

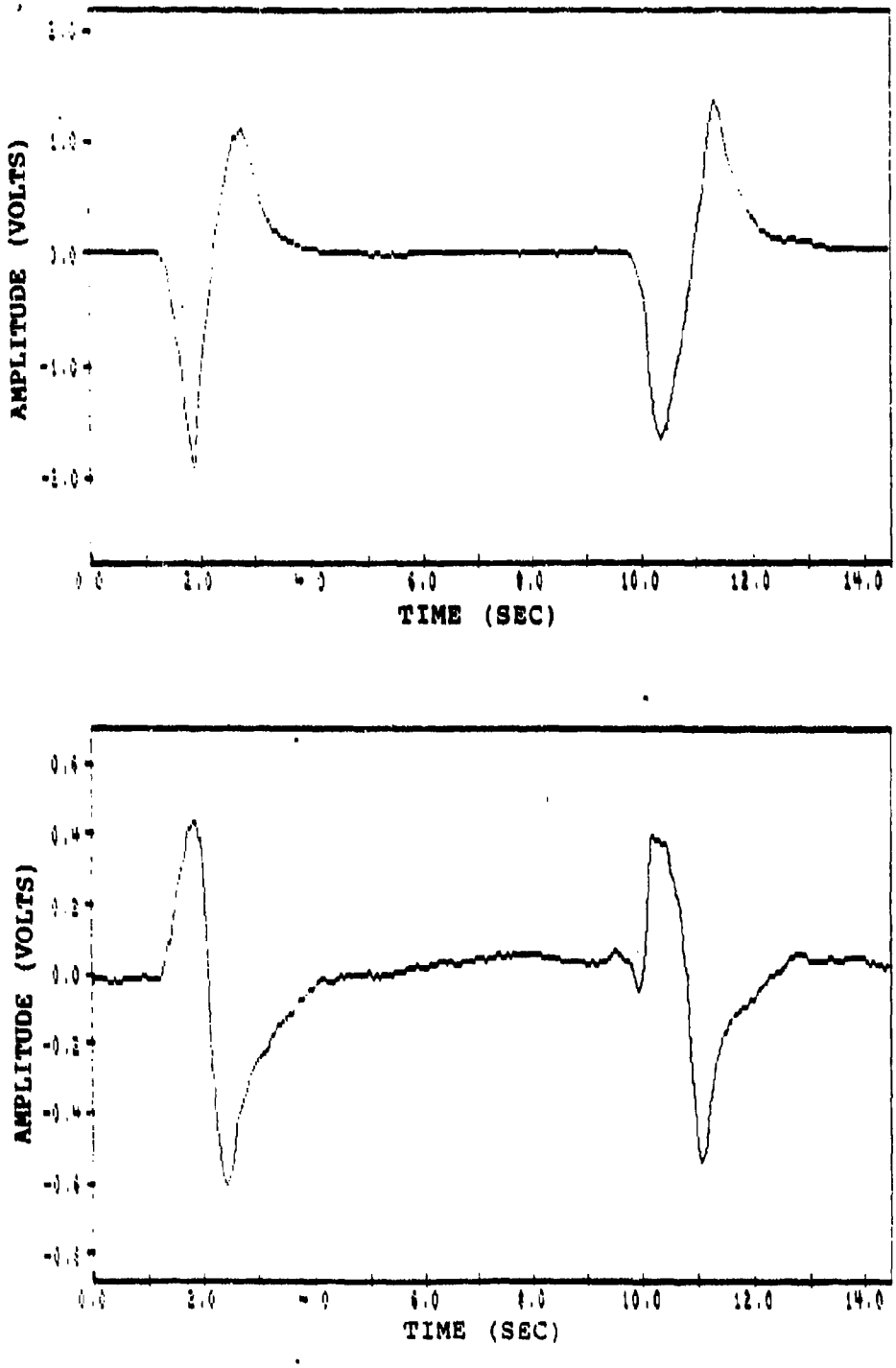

Figure 27. Bite/Grit Teeth Two Times; Left Channel (top), Right Channel (bottom)

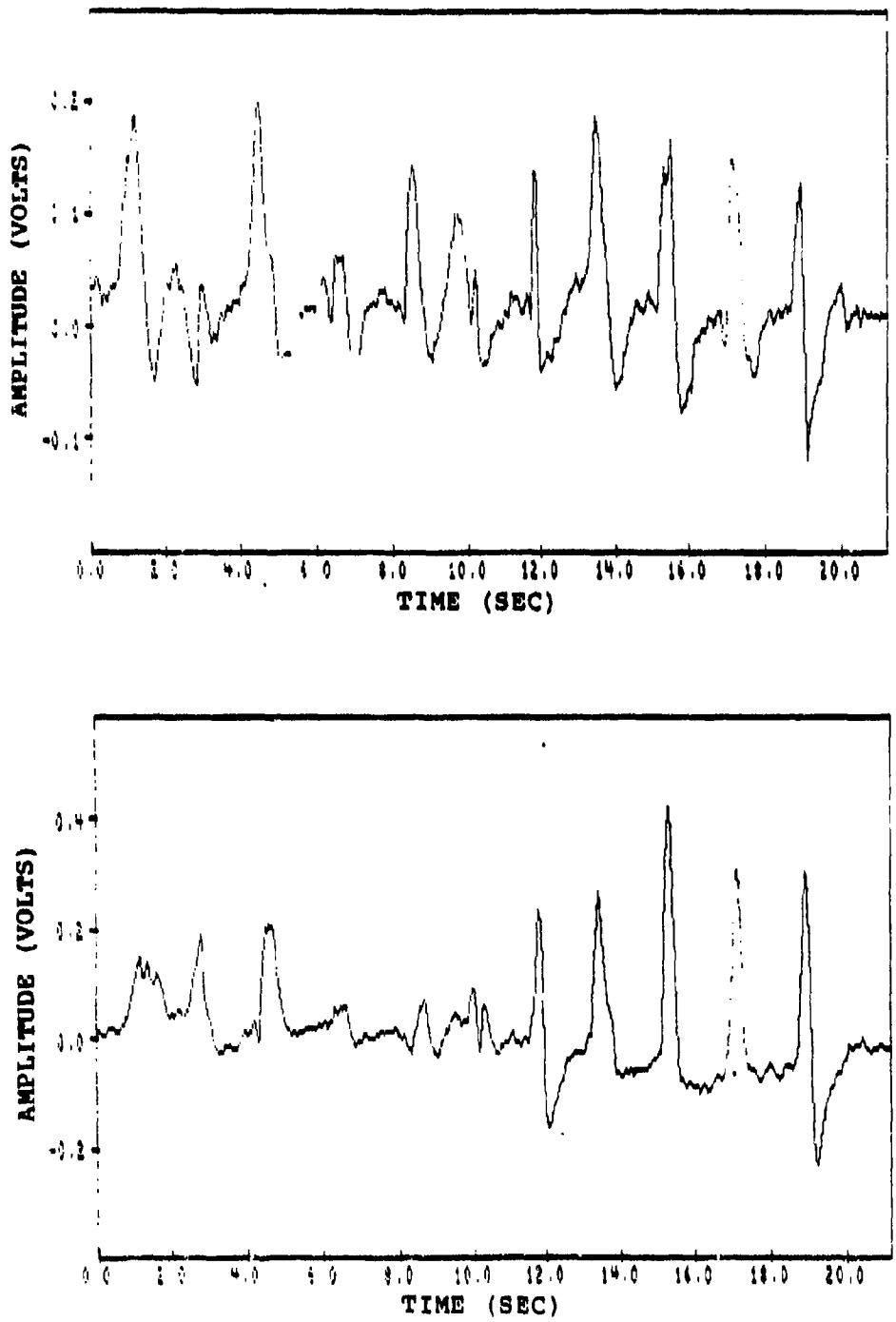

Figure 28. Count To Ten; Left Channel (top)
Right Channel (bottom)

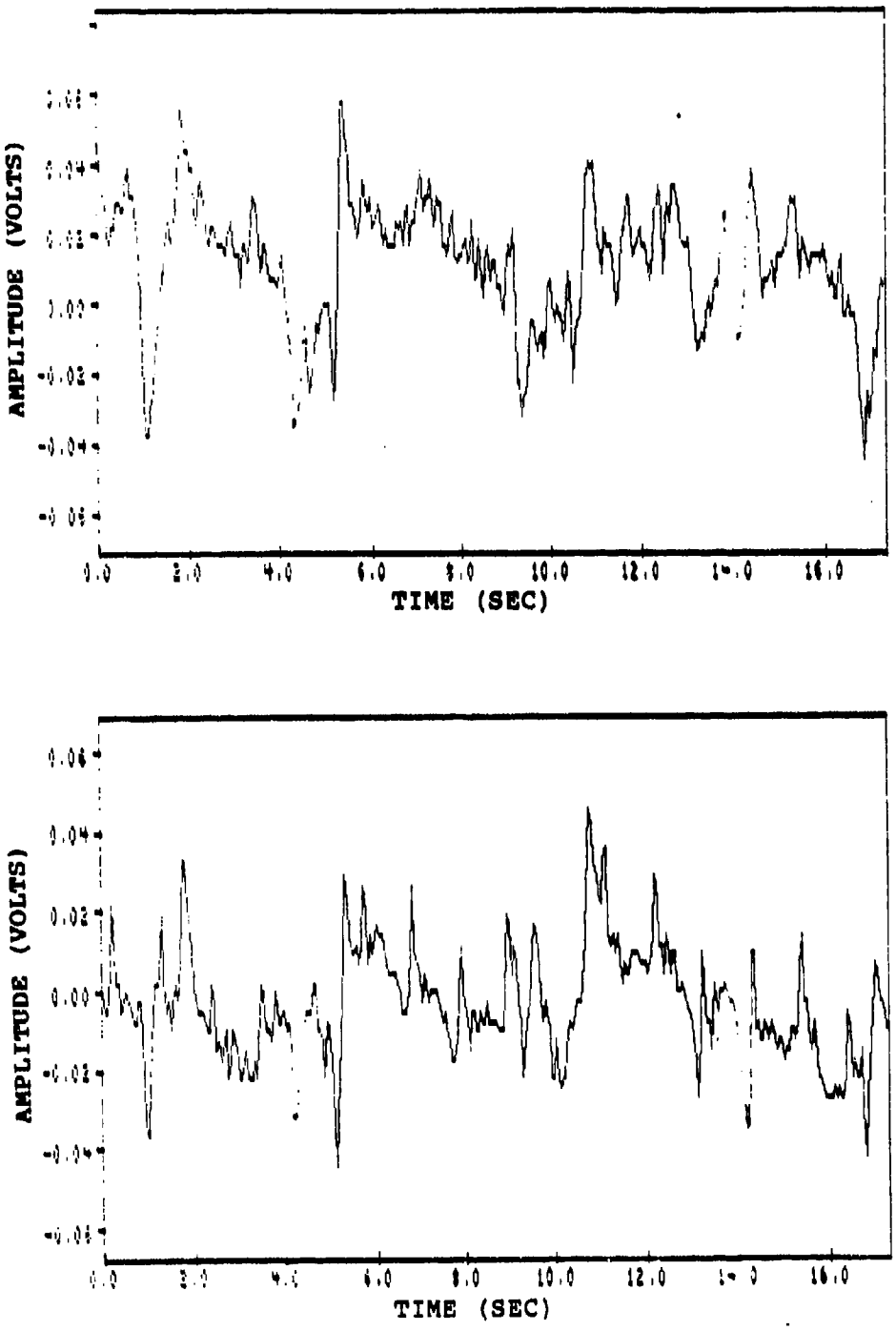

Figure 29. Face Flex Five Times; Left Channel (top), Right Channel (bottom)

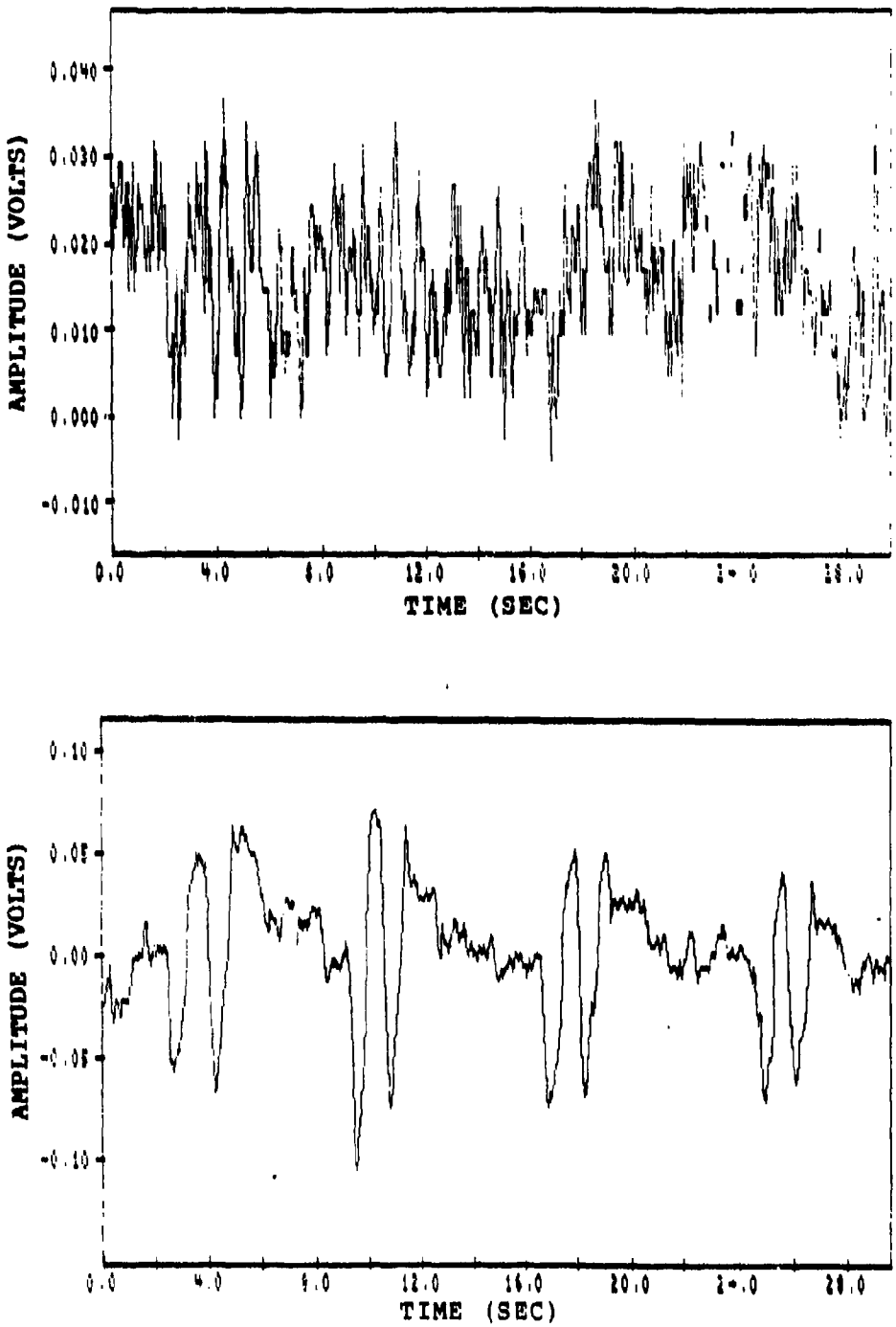

Figure 30. Level-Up-Level Eye Movement Four Times; Left Channel (top), Right Channel (bottom)

Appendix D

Example Sensor Test Data Run

The following seven pages contain an example of a sensor test data run recorded from a single pulse monitor. The data provided was collected from a the right temporal Region 3 of a test subject. The first figure shows a nine second example of a negative going pulse signal recorded during the absence of muscular movement. Peak amplitude of the pulse signal is approximately -0.12v. Subsequent figures show the same type of pulse signal from the first figure recorded during various types of muscular movement. These figures are a representative sample of signal-plus-noise data and are included here to provide a comparison between the pulse monitor signal and the amplitude levels for various noise artifacts.

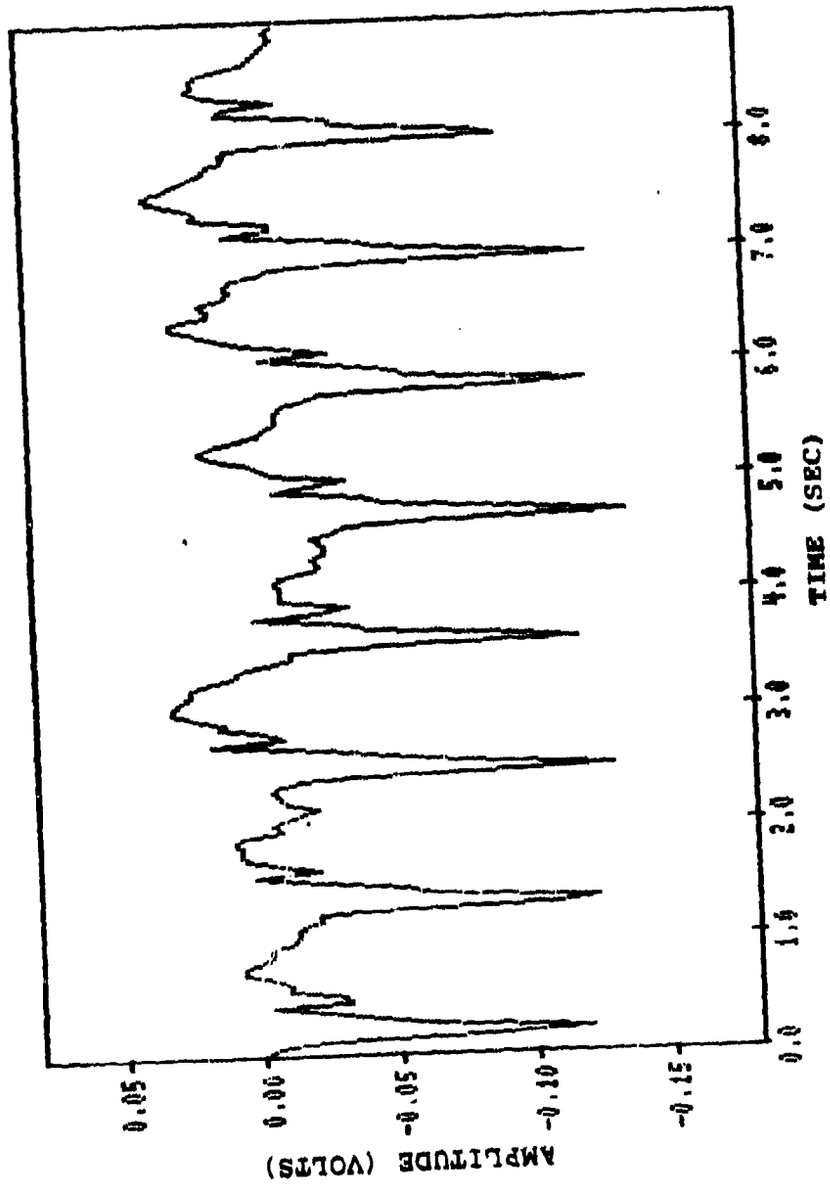

Figure 31. Negative Going Pulse Signal

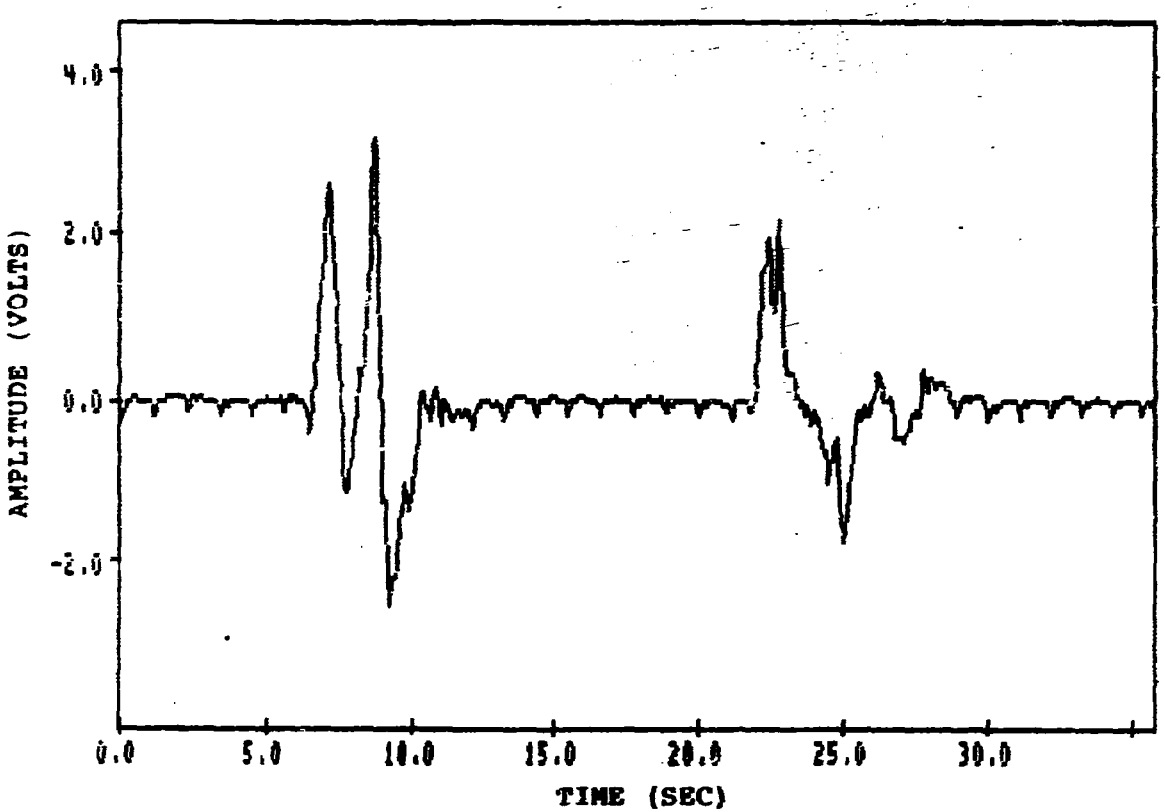

Figure 32. Signal Plus Two Yawns

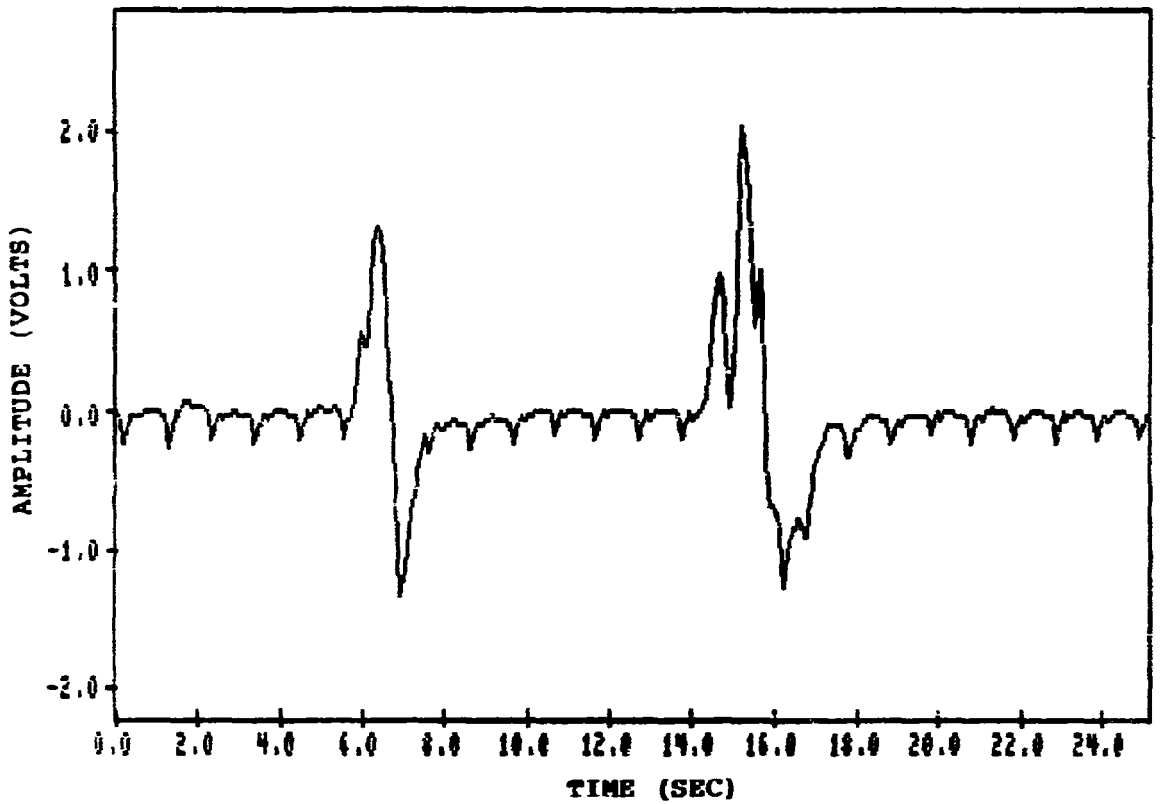

Figure 33. Signal Plus Two Swallows

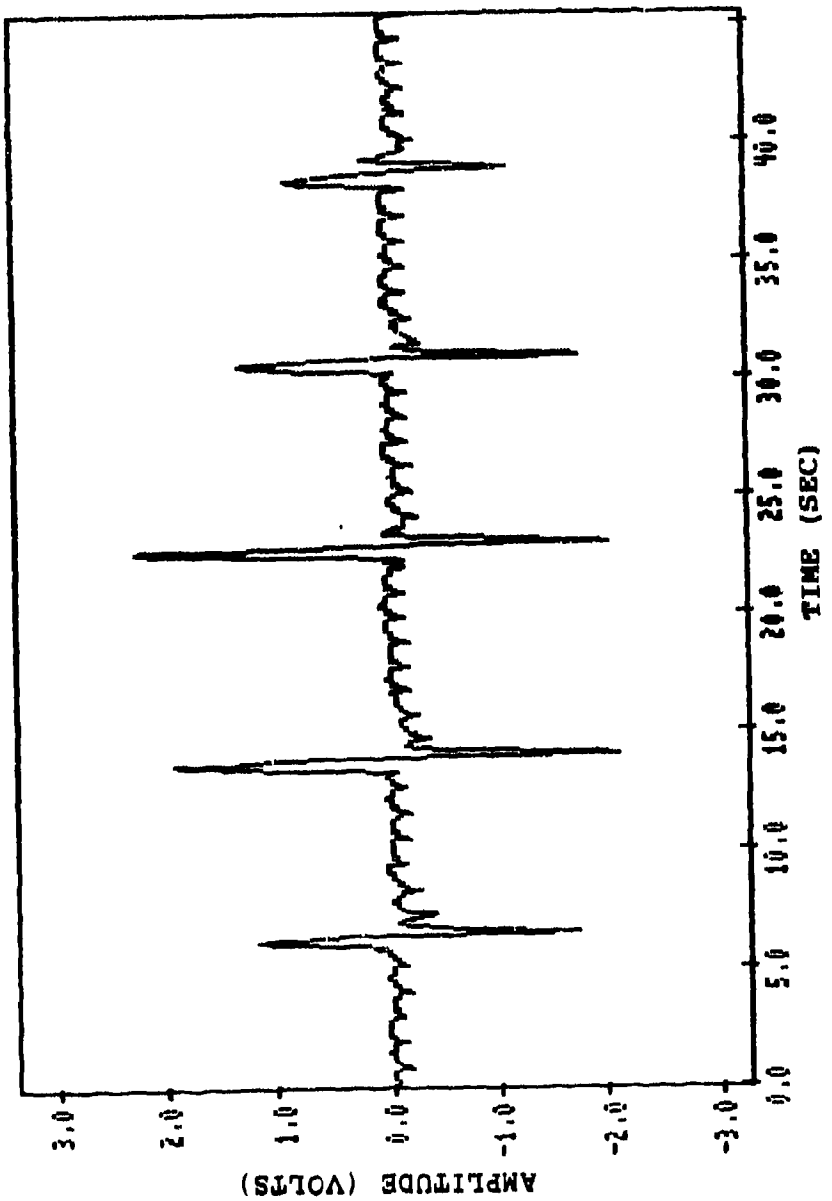

Figure 34. Signal Plus Open/Close Mouth Five Times

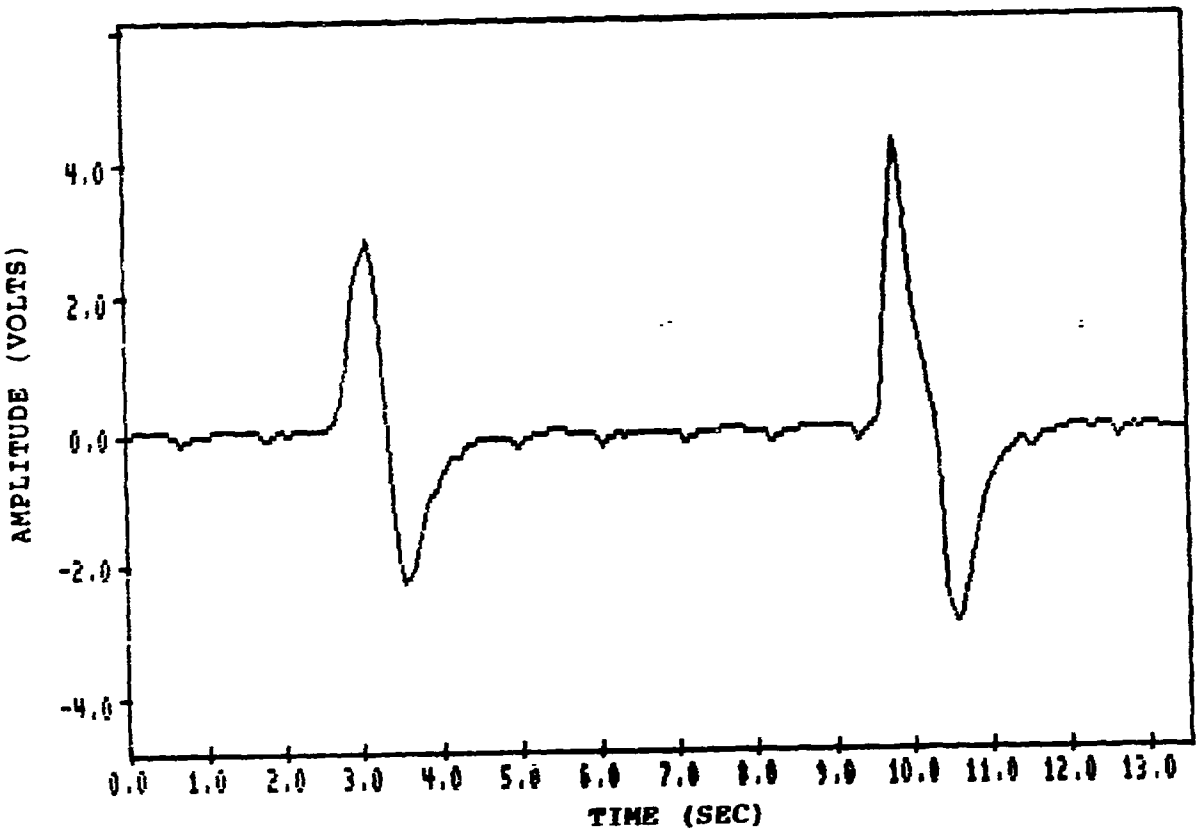

Figure 35. Signal Plus Bite/Grit Teeth Two Times

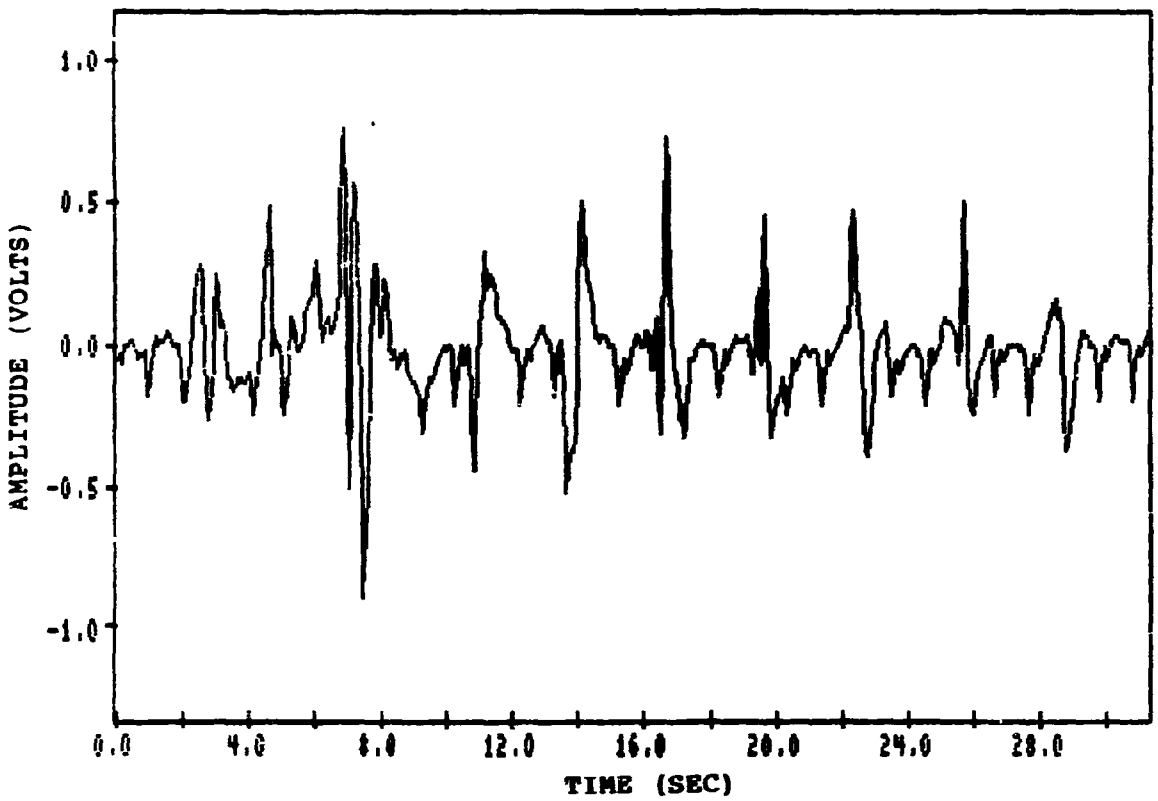

Figure 36. Signal Plus Counting To Ten

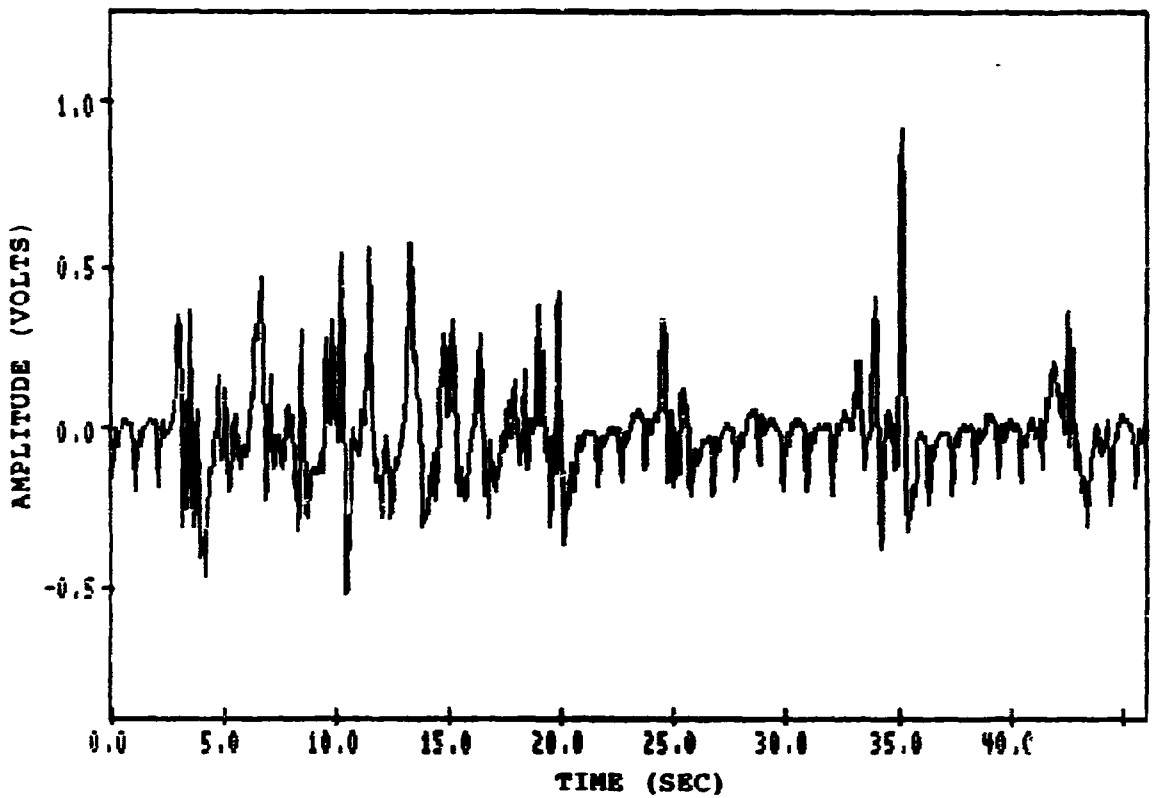

Figure 37. Signal Plus Reading

Appendix E

The following four pages contain the LMS adaptive noise cancellation filter program used in this thesis. This program was written using Turbo Pascal V4.0 and requires a 80287 math coprocessor chip to compile and run properly.

```
{$N+}

PROGRAM LMS_3C;

{       PROGRAM TITLE:  LMS ADAPTIVE NOISE CANCELLATION FILTER
        VERSION:  9SEP88
        AUTHOR:  CAPT BRIAN J. SIMES

        DESCRIPTION:  This program implements a 2 to 65 weight
        adaptive noise cancellation filter using the LMS
        algorithm.  Data input file lengths are limited to
        12000 data points.  This program requires an 80287
        math coprocessor and Turbo Pascal V4.0 to compile and
        run properly.  CTRL BREAK can be used to terminate
        execution of this program.

        INPUTS:  Two numeric data files (S.DAT and N.DAT) in
        32 bit floating point format located on a floppy disk
        in "A" drive.  File S.DAT contains signal plus noise
        data and represents the desired "D" signal in the
        filter algorithm.  File N.DAT contains noise data
        correlated with the S.DAT's noise data and represents
        the "X" input data in the filter algorithm.  Program
        prompts user for "data run number" (output file name),
        number of filter weights and a "u" filter weight
        update value.

        OUTPUT:  One numeric data file (Exxx.DAT) in 32 bit
        floating point format downloaded to a floppy disk in
        "A" drive.  File Exxx.DAT contains signal output
        (hopefully) and represents the error signal in the
        filter algorithm.  A monitor output containing (from
        left to right) by column:  data point number, error
        value, and filter weights W0, W1, W2 and W3.}

USES
   CRT, PRINTER;

CONST
   DataSizeMax = 11999;  {Limits number of data points in
                          input files; 10 minutes of data if
                          sample rate is 20 Hz.}

TYPE
   DataArray = ARRAY[0..DataSizeMax] OF SINGLE;
   Data = ^DataArray;
   FileNumber = STRING[3];
```

```
VAR
   WeightNumber, Clock, FilterSize  :INTEGER;
   PointerStart  :^SINGLE;
   u, Error, Noise_Y, Signal  :SINGLE;
   E, N, S, W  :FILE OF SINGLE;
   Noise_X  :Data;
   Weight  :ARRAY[0..64] OF SINGLE;
   DataRunNumber  :FileNumber;
   CheckBreak  :BOOLEAN;


PROCEDURE Clear_Space;

BEGIN
   GOTOXY(1,22); CLREOL;
   GOTOXY(1,23); CLREOL;
   GOTOXY(1,24); CLREOL;
END;


PROCEDURE Get_Filter_Constants;

BEGIN
   CLRSCR;
   GOTOXY(1,22);
   WRITE('Enter data run number (use a number between 000
   and 999).   >');
   READ(DataRunNumber);
   CLRSCR;
   GOTOXY(1,22);
   WRITE('Enter number of weights in filter (2 to 65).  >');
   READ(FilterSize);
   FilterSize:=(FilterSize-1);
   CLRSCR;
   GOTOXY(1,22);
   WRITELN('Enter value of "u" (0 to 1).... ');
   WRITE('(i.e., 0.54 for .54 etc.).  >'); READ(u);
END;


PROCEDURE Initialize_Data_Arrays;

BEGIN
   FOR WeightNumber:=0 TO FilterSize DO
   BEGIN
      Weight[WeightNumber]:=0;   {Set all weights to zero
                                  initially.}
   END;
END;
```

```
PROCEDURE Run_Filter;

BEGIN
   Clear_Space;
   ASSIGN(S,'A:S.DAT');
   RESET(S);
   ASSIGN(N,'A:N.DAT');
   RESET(N);
   MARK(PointerStart);
   NEW(Noise_X);
   ASSIGN(E,CONCAT('A:E',DataRunNumber,'.DAT'));
   REWRITE(E);
   Clock:=0;
   WHILE NOT EOF(S) DO
   BEGIN
      READ(S,Signal);
      READ(N,Noise_X^[Clock]);  write(clock:8);
      Noise_Y:=0;

{Calculate first output data point of filter}

      IF Clock=0 THEN
      BEGIN
         Error:=Signal;
         WRITE(E,Error);   WRITELN('   E =',Error:9:4,'   ',
         Weight[0]:9:4,'   ',Weight[1]:9:4,
         '   ',Weight[2]:9:4,'   ',Weight[3]:9:4);
         Clock:=Clock+1;
      END ELSE
      BEGIN

{Calculate output data points while filter is loaded up with
data}

         IF (Clock-FilterSize)<=0 THEN
         BEGIN
                  FOR WeightNumber:=0 TO Clock-1 DO
            BEGIN
               Weight[WeightNumber]:=Weight[WeightNumber]+
               2*u*Error*Noise_X^[(Clock-1-WeightNumber)];
               Noise_Y:=Noise_Y+Weight[WeightNumber]*
               Noise_X^[Clock-WeightNumber];
            END;
            Error:=Signal-Noise_Y;
            WRITE(E,Error);    WRITELN('   E =',Error:9:4,
            '   ',Weight[0]:9:4,'   ',Weight[1]:9:4,
            '   ',Weight[2]:9:4,'   ',Weight[3]:9:4);
            Clock:=Clock+1;
         END ELSE
```

```
          BEGIN

{Calculate output data points after filter is initially
loaded with data}

              FOR WeightNumber:=0 TO FilterSize DO
              BEGIN
                 Weight[WeightNumber]:=Weight[WeightNumber]+
                 2*u*Error*Noise_X^[(Clock-1-WeightNumber)];
                 Noise_Y:=Noise_Y+Weight[WeightNumber]*
                 Noise_X^[Clock-WeightNumber];
              END;
              Error:=Signal-Noise_Y;
              WRITE(E,Error);    WRITELN('   E =',Error:9:4,
              '   ',Weight[0]:9:4,'   ',Weight[1]:9:4,
              '   ',Weight[2]:9:4,'   ',Weight[3]:9:4);
              Clock:=Clock+1;
            END;
       END;
    END;
    RELEASE(PointerStart);
    CLOSE(S);
    CLOSE(N);
    CLOSE(E);
END;


{***** MAIN PROGRAM *****}

BEGIN
      TEXTCOLOR(WHITE);
      TEXTBACKGROUND(BLUE);
      Get_Filter_Constants;
      Initialize_Data_Arrays;
      Run_Filter;
END.
```

Bibliography

1. Bershad, Neil J. "On Error-Saturation Nonlinearities in LMS Adaption," IEEE Transactions On Acoustics, Speech, and Signal Processing, 36: 440-452 (April 1988).

2. -----. "On the Optimum Gain Parameter in LMS Adaption," IEEE Transactions On Acoustics, Speech, and Signal Processing, 35: 1065-1068 (July 1987).

3. Burr-Brown Integrated Circuits Data Book. 2-26 (June 1986).

4. Clemente, Carmine D. Anatomy: A Regional Atlas of the Human Body (Third Edition). Baltimore: Urban and Schwarzenberg Inc., 1987.

5. Mawhinney, Daniel D. Final Report Multiple Sensor Arterial Pulse Monitor. Contract F33615-85-C-0530. Princeton NJ: RCA Laboratories, David Sarnoff Research Center, 1988.

6. -----. Flight Helmet Instrumented with Multiple Arterial Pulse Sensors. Princeton NJ: MMTC, Inc., 1988.

7. Mawhinney, Daniel D. and Milgazo, Henry F. "A Miniaturized Microwave Sensor for Monitoring the Superficial Temporal Arterial Pulse," NAECON 87, (May 1987).

8. Mawhinney, Daniel D. and Kresky, Thomas. Superficial Temporal Artery Monitor. Contract F33615-81-C-0500. Princeton NJ: RCA Laboratories, David Sarnoff Research Center, March 1986 (AAMRL-TR-86-008).

9. -----. "Non-Invasive Physiological Monitoring with Microwaves," NAECON 86. 746-751 (May 1986).

10. Medical Systems Laboratory. Arterial Pulse Monitor. Model S587B. RCA Laboratories, David Sarnoff Research Center, Princeton NJ, 1988.

11. RCA Laboratories. Final Report Miniaturized Superficial Temporal Artery Monitor. Contract F33615-81-C-0530. Princeton NJ: 1986.

12. Skylar, Bernard. Digital Communications Fundamentals and Applications. New Jersey: Prentice Hall, 1988.

13. Van Patten R.E. "Current Research on an Artificial Intelligence-based Loss of Consciousness Monitoring System for Advanced Fighter Aircraft," NAECON 87. 1000-1004 (May 1987).

14. -----. "A Methodology for the Reduction of False Alarm Rates In Artificial Intelligence-Based Loss of Consciousness Monitoring Systems," NAECON 88. 881-884 (May 1988).

15. Widrow, Bernard and Stearns, Samuel D. Adaptive Signal Processing. New Jersey: Prentice Hall, 1985.

16. Widrow, Bernard and Walach, Eugene. "On the Statistical Efficiency of the LMS Algorithm with Nonstationary Inputs," IEEE Transactions on Information Theory 30: 211-221 (March 1984).

17. Widrow, Bernard and others. "Stationary and Nonstationary Learning Characteristics of the LMS Adaptive Filter," Proceedings of the IEEE 64: 1151-1162 (August 1976).

18. -----. "Adaptive Noise Cancelling: Principles and Applications," Proceedings of the IEEE 63: 1692-1716 (December 1975).

VITA

Captain Brian J. Simes was born on 10 November 1957 in Cincinnati, Ohio. He graduated from Zweibruecken American High School, Zweibruecken Germany in 1976. He attended the Ohio State University from 1976 to 1981 and received a Bachelor of Science in Electrical Engineering degree in 1981. After graduating from college, he attended graduate school at the Ohio State University and was a bio-medical engineer student intern in the Grant Hospital Vascular Lab from 1981 to 1982. Upon completion of his internship, he attended the United States Air Force Officer Training School where he was commissioned into the USAF. He worked as a engineer and test manager in the Deputy for Range Systems from 1983 to 1987 at the Armament Division, Air Force Systems Command, Eglin AFB, Florida. Captain Simes entered the Masters Program at the Air Force Institute of Technology, Wright-Patterson AFB, Ohio in May 1987.

Permanent Address: 668 Edmonds Drive
Charleston, SC 29412

UNCLASSIFIED

SECURITY CLASSIFICATION OF THIS PAGE

REPORT DOCUMENTATION PAGE

Form Approved OMB No. 0704-0188

1a. REPORT SECURITY CLASSIFICATION UNCLASSIFIED	1b. RESTRICTIVE MARKINGS
2a. SECURITY CLASSIFICATION AUTHORITY	3. DISTRIBUTION/AVAILABILITY OF REPORT Approved for public release; distribution unlimited
2b. DECLASSIFICATION/DOWNGRADING SCHEDULE	
4. PERFORMING ORGANIZATION REPORT NUMBER(S) AFIT/GE/ENG/88D-45	5. MONITORING ORGANIZATION REPORT NUMBER(S)
6a. NAME OF PERFORMING ORGANIZATION School of Engineering 6b. OFFICE SYMBOL (If applicable)	7a. NAME OF MONITORING ORGANIZATION
6c. ADDRESS (City, State, and ZIP Code) Air Force Institute of Technology (AU) Wright-Patterson AFB, OH 45433-6583	7b. ADDRESS (City, State, and ZIP Code)
8a. NAME OF FUNDING/SPONSORING ORGANIZATION Acceleration-Effects Branch 8b. OFFICE SYMBOL (If applicable) AAMRL/BBS	9. PROCUREMENT INSTRUMENT IDENTIFICATION NUMBER
8c. ADDRESS (City, State, and ZIP Code) Armstrong Aerospace Medical Research Lab Wright-Patterson AFB, OH 45433	10. SOURCE OF FUNDING NUMBERS PROGRAM ELEMENT NO. / PROJECT NO. / TASK NO / WORK UNIT ACCESSION NO.

11. TITLE (Include Security Classification)
LMS Adaptive Filtering Applied to a Microwave Arterial Pulse Monitor (Unclassified)

12. PERSONAL AUTHOR(S)
Brian J. Sirmas, B.S.E.E., Captain, USAF

13a. TYPE OF REPORT	13b. TIME COVERED	14. DATE OF REPORT (Year, Month, Day)	15. PAGE COUNT
MS Thesis	FROM ____ TO ____	1988 December	117

16. SUPPLEMENTARY NOTATION

17. COSATI CODES			18. SUBJECT TERMS (Continue on reverse if necessary and identify by block number)
FIELD	GROUP	SUB-GROUP	Adaptive Filter, Filter, Microwave, Monitor
06	12		

19. ABSTRACT (Continue on reverse if necessary and identify by block number)

A prototype microwave arterial pulse monitor was evaluated and modified. Evaluation test data was collected from the temporal region of human volunteers using the microwave arterial pulse monitor. Three sets of test signals were developed using this test data. These test signals were used to evaluate the feasibility of using a LMS adaptive noise cancellation filter for reduction of noise artifacts observed in the output of the microwave arterial pulse monitor.

A computer program using the LMS algorithm was written and the performance of the LMS filter was evaluated for its effectiveness in removing unwanted noise. A system model describing the performance characteristics of the test subject-monitor-filter interface is presented.

Approved for public release: IAW AFR 190-1
JOSEPH P. HIPPS
Dean for Research and Professional Development
AFIT, Wright-Patterson AFB OH 45433-6583
12 Jan 89

20. DISTRIBUTION/AVAILABILITY OF ABSTRACT	21. ABSTRACT SECURITY CLASSIFICATION
☒ UNCLASSIFIED/UNLIMITED ☐ SAME AS RPT. ☐ DTIC USERS	UNCLASSIFIED
22a. NAME OF RESPONSIBLE INDIVIDUAL Robert Williams, Captain, USAF	22b. TELEPHONE (Include Area Code) (513) 255-6027
	22c. OFFICE SYMBOL AFIT/ENG

DD Form 1473, JUN 86 — Previous editions are obsolete. — SECURITY CLASSIFICATION OF THIS PAGE
UNCLASSIFIED